

RSC Advances



This is an *Accepted Manuscript*, which has been through the Royal Society of Chemistry peer review process and has been accepted for publication.

Accepted Manuscripts are published online shortly after acceptance, before technical editing, formatting and proof reading. Using this free service, authors can make their results available to the community, in citable form, before we publish the edited article. This *Accepted Manuscript* will be replaced by the edited, formatted and paginated article as soon as this is available.

You can find more information about *Accepted Manuscripts* in the [Information for Authors](#).

Please note that technical editing may introduce minor changes to the text and/or graphics, which may alter content. The journal's standard [Terms & Conditions](#) and the [Ethical guidelines](#) still apply. In no event shall the Royal Society of Chemistry be held responsible for any errors or omissions in this *Accepted Manuscript* or any consequences arising from the use of any information it contains.

Bovine Glutamate Dehydrogenase Immobilization on Magnetic Nanoparticles : conformational changes and catalysis

Caterina G. C. Marques Netto ^{*a,b}, Delmácio G. da Silva ^b, Sergio H. Toma ^b, Leandro H. Andrade^c, Marcelo Nakamura ^b, Koiti Araki ^b, Henrique E.Toma ^b

a- Present Address: Metalloenzymes and Mimetics Laboratory, UFSCar, São Carlos-SP, Brazil

b- Supramolecular NanotechLab, Instituto de Química, Universidade de São Paulo, São Paulo—SP, Brazil

c- Laboratory of Fine Chemistry and Biocatalysis, Instituto de Química, Universidade de São Paulo, São Paulo—SP, Brazil

e-mail: caterina@ufscar.br

Abstract

Glutamate dehydrogenase (GDH) is a well known homohexameric enzyme and its performance in immobilized form was systematically investigated in this work, in order to provide a better understanding of the multimeric enzyme immobilization effects in relation to the monomeric ones. For this purpose, GDH was immobilized on four different magnetic supports and the outcome from such immobilization was characterized in terms of their stabilization and activity. Immobilization procedures involving amine coupling *via* glutaraldehyde cross-linking yielded the least stable ones, even lower than free GDH, showing no recoverability. However, the immobilization procedures using larger aldehyde cross-linkers presented higher thermal stabilities than free GDH and could be recycled at least 10 times, with a nearly constant activity. Such differences in stability and activities were thoroughly evaluated in terms of the enzymatic structure, which has guided the reasoning behind the intriguing allosteric behavior of the immobilized GDH. The atypical allosteric response exhibited by MagNP-APTS/GDH, MagNP@SiO₂-APTS/GDH and MagNP-APTS/Glyoxyl-Agarose/GDH led us to invoke the intrinsic disorder theory to explain the results. This theory has proved an excellent tool to guide researches on immobilized enzymes and understand its effects.

Keywords: Glutamate dehydrogenase, Immobilization, Ensemble theory

Introduction

Enzyme immobilization is a technique used to obtain recoverable, stable and in several cases, to generate a system with higher activities than the free protein^{1,2}. The properties of an immobilized biocatalyst are related to the methodology and supporting material employed, but they also depend on the amino acid composition of the enzyme's surface³. However, despite of the extensive studies reported in this area⁴, the resulting enzyme activity is not easy to predict⁵ and a previous knowledge of the catalysis is essential for the comprehension of the new system resulting from the protein anchoring to a support⁶. Considering that the catalytic properties of an enzyme are intimately dependent on the protein's three-dimensional conformation and the keyhole-lock relationship between enzyme and substrate⁷, it is foreseen that any perturbation of the protein's native configuration will impact its activity;^{3a,8}

In general, an impact on the enzymatic activity upon immobilization is determined by the induction of microenvironment and conformational changes⁹ and the extent of impact suffered by a multimeric enzyme after immobilization is expected to be larger than for monomeric ones.¹⁰ The greater impact on multimeric enzymes can be related to enzyme subunit dissociation¹⁰⁻¹¹ or to disturbance in the subunits interactions in the quaternary structures after fixation on a support.¹² Therefore, multimeric enzyme immobilization is a rather complex problem since overcoming the issues about enzyme stabilization^{13,14} includes a supporting material design^{3b,10,12b,15,16} and study of immobilization procedures.^{8b,17,18}

Another issue faced by multimeric enzymes immobilization is the disturbance of allosteric mechanisms. Some proteins are ordered or disordered prior to ligand binding in other parts of the molecule, regulating a long-range allosteric interaction within the protein.^{19,20} As a consequence, any modification of these mechanisms through immobilization can alter the precise distribution of states within the native state ensemble^{21,22} and modulate the allosteric response of the whole system. An example of a useful multimeric enzyme is the 336 kDa homohexameric protein glutamate dehydrogenase (GDH) from bovine liver,^{23,24} which has its activity tightly controlled by a complex network of allosteric regulators^{23,25} and its immobilization can induce differences in allosteric response.²⁶ In its immobilized form, glutamate dehydrogenase is normally used as glutamate probes,²⁷⁻³⁰ employing different supports and methodologies for the attachment on a support.^{12b,26c,29,31} However, regardless of

the extensive amount of study on GDH immobilization, the use of magnetic nanoparticles is still in early stages.³²

Therefore, bearing the challenge of obtaining a reusable and stable multimeric biocatalyst^{12a,33} and the demand of GDH stabilization and activation^{24,34}, we performed the immobilization of glutamate dehydrogenase on magnetite nanoparticles (MagNP) displaying different characteristics. Aminopropyltriethoxysilane (APTS) was used as a surface modifier³⁵ in two different supports: one with no silica shell and the other one with a silica shell (MagNP-APTS and MagNP@SiO₂-APTS), employing glutaraldehyde as a cross-linking agent.³⁶ Differences in enzymatic activities between these two supports would be mainly due to iron exposure to the protein's surface.³⁷ Glyoxyl-carboxymethylcellulose and glyoxyl-agarose³⁸ were the other two cross-linking agents chosen (MagNP@CMC and MagNP-APTS-Glyoxyl-Agarose), both exhibit a higher loading of aldehyde groups that can help to afford high enzyme loadings, but can also interfere in the catalytic reaction by greater diffusional limitations of the substrates.^{1,3b,4,5,11a,39} Consequently, beyond the advantage of easy recoverability of magnetic nanoparticles by the use of an external magnetic field,^{40,41} the difference between these immobilization protocols in stabilization, activation and allostereism should also be investigated. In this work, it became evident that different supports can yield contrasting GDH properties, with higher or lower stability and activity, depending on the enzyme-attachment methodology. The intrinsic disorder mechanism^{19a} was employed for each immobilized system and proved to be an important tool for understanding the effect of different immobilization protocols on the enzyme behavior.

Experimental Section

All reagents were purchased from Sigma-Aldrich and were used without previous purification. Glutamate dehydrogenase (type II) from bovine liver exhibited ≥ 35 units/mg of protein (one unit expresses the reduction of 1 μmol of α -ketoglutarate to L-glutamate per minute in the presence of NADH (2.4 mmol L⁻¹) and ammonium ions at pH 7.3 and 25 °C). Trypsin used in tryptic digestion was TPCK treated from bovine pancreas, exhibiting $\geq 10,000$ Benzoyl-L-arginine ethyl ester (BAEE) units/mg protein (One BAEE unit will produce a A₂₅₃ of 0.001 per minute at pH 7.6 at 25°C using BAEE as a substrate. One BTEE unit = 320 ATEE unit).

Synthesis of MagNP-APTS, MagNP@SiO₂-APTS and MagNP@CMC

The synthesis of MagNP-APTS and MagNP@SiO₂-APTS has been described elsewhere.^{37,42} The MagNP@CMC material was generated from freshly prepared magnetic nanoparticles by treating with 0.5 % aqueous alkaline solution of carboxymethyl-cellulose (CMC), pH 12, under stirring and reflux for 30 min. The nanoparticles were magnetically concentrated, and washed with deaerated water, yielding stable colloidal solutions displaying average global particle size of 90 nm (based on DLS) and magnetic core of about 25 nm (SEM). MagNP@CMC particles were further dried at 100 °C for 12 hours. Activation of the hydroxyl groups from the CMC shell was performed by suspending 500 mg of MagNP@CMC in 3 mL of deionized water, followed by the addition of 250 μL of 2 mol L⁻¹ NaOH solution (containing 6.7 mg of NaBH₄) at 0°C. Then, 180 μL of glycidol was added dropwise and the reaction proceeded for additional 16 hours at room temperature. The particles were then washed with water (3x 10 mL) and 15 mg of NaIO₄ dissolved in 5 mL of water was added. The reaction proceeded for 3 hours and after that period, the particles were washed with water (10x 10 mL) and kept in suspension (200 mg/mL).

General procedure of GDH immobilization on MagNP-APTS

MagNP-APTS (0, 1, 2, 4, 8 and 16 mg) suspended in 100 μL of TRIS-HCl buffer solution (pH 7.5, 0.1 mol L⁻¹) was mixed with 100 μL of a GDH solution (0.523 mg/mL, 2 U in 0.1M Tris-HCl buffer pH 7.5). To this mixture glutaraldehyde (0, 2, 5, 10 and 15 μL of a 0.2% solution in water) was added and the suspension was stirred at 120 rpm for 5, 10, 15 or 20 minutes, at 0 °C. The immobilized enzymes were confined by using an external miniature Nd₂Fe₁₄B magnet (1 cm³, 11 kOe from MagTek), and washed 3 times with 0.1 mL of TRIS-HCl buffer solution (pH 7.5, 0.1 mol L⁻¹). The best immobilization conditions were obtained by using 2 mg of MagNP-APTS, 2 μL of a glutaraldehyde solution and stirring for 5 minutes, which afforded the system MagNP-APTS/GDH. (Amount of immobilized GDH: 0.05 mg/2 mg MagNP-APTS).

General procedure of GDH immobilization on MagNP@SiO₂-APTS

MagNP@SiO₂-APTS (0.6, 1.2, 2.4, 4 and 8 mg) suspended in 100 μL of TRIS-HCl buffer solution (pH 7.5, 0.1 mol L⁻¹) was mixed with 100 μL of a GDH solution 0.523 mg/mL (2 U). Then, glutaraldehyde (0, 2, 5, 10 and 15 μL of a 0.2% solution in water) was added and the resulting mixture was stirred at 120 rpm for 2.5, 5, 10 or 15 minutes, at 0 °C. The immobilized enzymes were confined by using an external miniature Nd₂Fe₁₄B magnet, and washed 3 times with 0.1 mL of TRIS-HCl buffer solution (pH 7.5, 0.1 mol L⁻¹). The best immobilization conditions

were obtained by using 1.2 mg of MagNP@SiO₂-APTS and 10 μL of a glutaraldehyde solution and stirring time of 5 minutes, which afforded the system MagNP@SiO₂-APTS/GDH. (Amount of immobilized GDH: 0.05 mg/1.2 mg MagNP@SiO₂-APTS).

General procedure of GDH immobilization on MagNP-APTS/Glyoxyl-Agarose

MagNP-APTS (1, 2, 4, 8 and 12 mg) suspended in 100 μL of TRIS-HCl buffer solution (pH 7.5, 0.1 mol L⁻¹) was mixed with 100 μL of a GDH solution 0.523 mg/mL (2 U). Then a 150 mg/mL suspension of glyoxyl-agarose (10, 25, 50, 125 and 150 μL) was added to the enzyme-nanoparticle mixture and the resulting mixture was stirred at 120 rpm at 0 °C for 2, 5, 10 or 20 minutes. The immobilized enzymes were confined by using an external miniature Nd₂Fe₁₄B magnet, and washed 3 times with 0.1 mL of TRIS-HCl buffer solution (pH 7.5, 0.1 mol L⁻¹). The best immobilization conditions were obtained by using 12 mg of MagNP-APTS, 50 μL of glyoxyl-agarose and stirring time of 5 minutes. The MagNP-APTS/Glyoxyl-Agarose/GDH material exhibited 0.05 mg of immobilized GDH for 12 mg of MagNP-APTS.

General procedure of GDH immobilization on MagNP@CMC

MagNP@CMC (10, 20, 30, 40 and 50 μL) from a 200 mg/mL stock suspension was mixed with a certain volume (50, 100, 150, 200 and 150 μL) of GDH solution (0.523 mg/mL, or 2 U in 0.1M Tris-HCl buffer pH 7.5). The resulting mixture was stirred at 120 rpm for 2.5, 5, 10 or 20 minutes, at °C. The immobilized enzymes were confined by using an external miniature Nd₂Fe₁₄B magnet, and washed 3 times with 0.1 mL of TRIS-HCl buffer solution (pH 7.5, 0.1 M). The best immobilization conditions were obtained by using 30 μL of MagNP@CMC suspension, 100 μL of the GDH solution and stirring time of 5 minutes. The MagNP@CMC/GDH material exhibited 0.05 mg of immobilized GDH for 2 mg of MagNP@CMC.

Enzyme Activity measurements

The as-prepared magnetic GDH were added to an optical quartz cuvette together with 20 μL of a 0.1 mol L⁻¹ glutamate solution, 50 μL of a 2.4 mmol L⁻¹ NAD⁺ solution and 900 μL of buffer solution. The activity was measured by monitoring the absorbance increase at 340 nm associated with the NADH formation at 25 °C. A fixed time of 10 minutes was maintained for all the reactions and the yields between each system were compared.

For the determination of the optimum pH, the experiments were performed at 25°C and for the optimum temperature, the experiments were performed at pH 7.5 (Tris-HCl buffer solution 0.1 mol L⁻¹)

Thermodynamic measurements

Determination of $S_{0.5}$ was performed at 25°C, pH 7.5 with 0.1 mol L⁻¹ Tris-HCl buffer solution, 50 µL of NAD⁺ (stock solution 0.9 mmol L⁻¹) and glutamate concentration from 0 to 5 mM. Measurements of ΔH^\ddagger and ΔS^\ddagger were performed at 20, 21, 22, 23 and 25°C and pH 7.5.

Trypsin (BRP, European Pharmacopoeia Reference Standard) digestion

The enzyme (free or immobilized) was washed three times with a 0.1 mol L⁻¹ phosphate buffer solution with pH 7 and 0.1 mol L⁻¹ EDTA. From this content, three aliquots were separated:

- a) 10 µL of the GDH solution/suspension together with 5 µL of trypsin (1 mg/100 µL)
- b) 10 µL of the GDH solution/suspension together with 0.1 mL of ADP (0.1 mol L⁻¹) and 5 µL of trypsin (1 mg/100 µL)
- c) 10 µL of the GDH solution/suspension together with 0.1 mL of GTP (0.1 mol L⁻¹) and 5 µL of trypsin (1 mg/100 µL)

The tubes were incubated at 25 °C for 12 h. The digestion content was analyzed by MALDI-TOF.

Physical Measurements

UV–visible (UV–Vis) spectra were recorded on a Hewlett Packard 8453-A diode- array spectrophotometer.

For the atomic force microscopy (AFM) measurements the samples were prepared by depositing 5 µL of the nanoparticle solution over mica (Ted Pella Inc.), and allowing it to dry in a clean laminar flow chamber. The AFM images were collected on a PicoSPM I microscope (Molecular Imaging, MI) with PicoScan 2100 (MI) controller coupled with MACMode (MI) unit for intermittent contact AFM, MAC Mode SFM, and magnetic force microscopy (MFM). Data acquisition was obtained using a PicoScan (MI) device with the scan rate between 0.5 and 1.0 Hz operating from 256 to 512 points per line. For the AFM and MACMode SFM measurements, silicon tips with high aspect ratio from *Nanosensors* and *Agilent* (Type II MACLevers, $k \sim 2.8$ N/m; $f \sim 60$ kHz) were employed. The MFM images were obtained using silicon tips with magnetic coating of PPP-MFMR model (*Nanosensors*, $k \sim 2.8$ N/m; $f \sim 60$ kHz), and operating with interleave mode enabled with the lift mode active from 25 nm to 100 nm. The magnetic domains were detected by using the phase contrast imaging.

Confocal Raman Spectroscopy measurements were recorded on a WITec Alpha 300R microscope equipped with a Nd:YAG laser ($\lambda = 532$ nm) and a Nikon objective (20x NA = 0.8).

Results

The supporting materials employed for glutamate dehydrogenase immobilization were composed of magnetite particles covered with: (A) aminopropyl-triethoxysilane (APTS), (B) silica and APTS, (C) glyoxyl-agarose and (D) glyoxyl- β -cellulose, as shown in Figure 1. Essentially, two groups were derived from these supports: (A), (B) involving the reaction of the amine groups with glutaraldehyde as cross-linking agent, and (C), (D) involving the direct reaction with the available aldehyde groups. In the first group (B) possesses a silica shell coating the magnetic nanoparticles and preventing the iron exposure at the surface, while (A) does not have this feature.³⁷ In the other group, support (C) is made of MagNP-APTS and glyoxyl-agarose, allowing several magnetic nanoparticles to attach to glyoxyl-agarose surface, while support (D) has glyoxyl- β -cellulose coating the magnetic nanoparticles. The reason of using a mixture of MagNP-APTS and glyoxyl-agarose in case C was related to the size of cross-linking agent used for the immobilization. Since glutaraldehyde is small, it permits a direct interaction between enzyme and nanoparticle, while a larger cross-linker should prevent it.

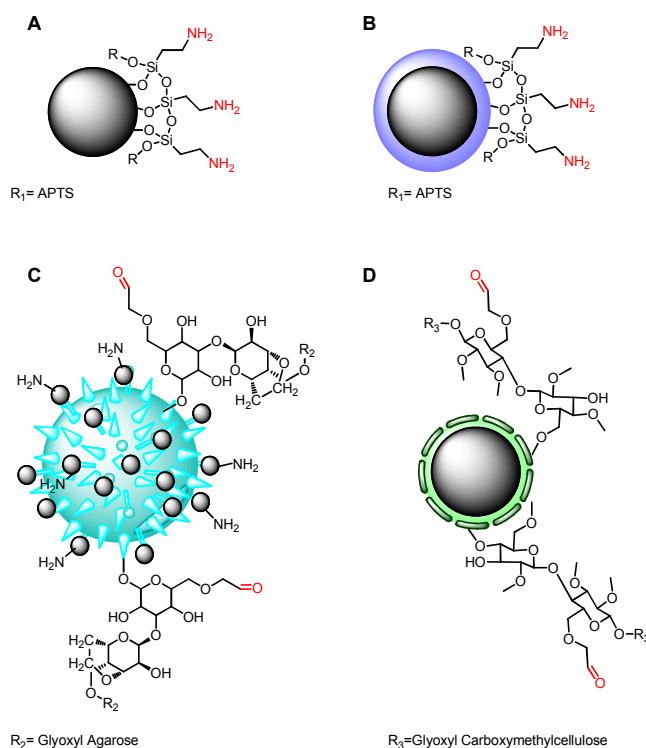


Figure 01. Schematic representation of the supports used for GDH immobilization. (A) MagNP-APTS, (B) MagNP@SiO₂-APTS, (C) MagNP-APTS/GlyoxylAgarose and (D) MagNP@CMC. The reactive groups are drawn in red.

A complete optimization of the immobilization protocols was performed, changing the amount of magnetic nanoparticles, cross-linking agent and reaction time (Support Information). The best protocols were chosen on the basis of the highest catalytic conversions for each methodology and were characterized according to their thermodynamic properties, pH-dependence, temperature-dependence, atomic force microscopy, recycling, allosteric response, Raman spectroscopy and tryptic digestion behavior. Before enrolling in the characterization, it should be noted that in any immobilization procedure, new interactions between enzyme and the components of the support can result from the immobilization, influencing its final conformation.^{43,44} This statement was confirmed by the thermodynamic properties shown in Table 1, in which, a significant decrease of ΔS^\ddagger and ΔH^\ddagger (calculated from the Eyring equation⁴⁵) is observed upon immobilization, in relation to free GDH [10,11] (Table 1, entry 1). The diminishment of ΔS^\ddagger can result from the protein-solvent interactions^{46,47}, e.g. from water molecules structuring around exposed hydrophobic aminoacid residues during catalysis⁴⁸ or either from an internal structure modification of the protein,⁴⁹ generating a rigid structure.⁵⁰ It is difficult to describe the exact mechanism responsible for lowering the ΔS^\ddagger in the immobilized GDH, but since immobilization fix the enzyme through several points available on a support, it is plausible that an overall stiffening is occurring. On the other hand, ΔH^\ddagger also decreases for all immobilized systems, as can be seen in Table 1, indicating a decrease in the temperature dependence of the enzyme in catalysis,⁵¹ as observed in Figure 3.

Likewise, distinct substrate affinity ($S_{0.5}$) is obtained after the immobilization procedures. For instance, by comparing the free and immobilized GDH, there is a noticeable increase in glutamate affinity for MagNP@SiO₂-APTS/GDH, MagNP-APTS/Glyoxyl-Agarose/GDH and MagNP@CMC/GDH in relation to free GDH as evidenced by a decrease in $S_{0.5}$ values in Table 1, whereas MagNP-APTS/GDH exhibits lower substrate affinity than free GDH (Table 1, entry 2).

Table 1. Values of $S_{0.5}$, ΔH^\ddagger , ΔS^\ddagger and n (Hill coefficient) for free and immobilized bovine liver GDH.

Entry	System	$S_{0.5}$ ($\mu\text{mol L}^{-1}$)	ΔH^\ddagger (kcal mol^{-1})*	ΔS^\ddagger (cal mol^{-1})*	N	K_{cat}^a (s^{-1})
1	Free GDH	190	34	110	2.1	0.12
2	MagNP-APTS/GDH	350	13	38	3.9	0.27

3	MagNP@SiO ₂ -APTS/GDH	75	16	50	3.5	0.19
4	MagNP-Glyoxyl Agarose/GDH	75	10	28	1.6	0.89
5	MagNP@CMC/GDH	15	8	25	1.2	1.21

* Per active site.

a- measured at 37°C and pH 6.8.

The multimeric enzyme system of GDH also includes subunits cooperativity and the extent of this cooperativity was compared using Hill coefficient (n , Table 1)⁵². Essentially, what is measured is an estimative of the affinity for other ligand molecules before and after immobilization, with $n > 1$ indicating a positive cooperativity, while $n = 1$ indicates no cooperativity.⁵³ Under the conditions of this work, free GDH presented n of 2.1, although after its immobilization on MagNP-APTS and MagNP@SiO₂-APTS the n value increased, indicating an enhanced positive cooperativity. However, in the case of MagNP@CMC and MagNP-APTS/Glyoxyl-Agarose, the enzyme modification seems to produce systems with almost no cooperativity, turning the n value very close to 1. This can be associated with the multi-point binding, promoted by the polymeric coating on the magnetic nanoparticles, preventing the enzyme dissociation and increasing the stability as observed by Garcia-Galan *et al.*^{12a} These features are also connected to the system thermal stability (Figure 2), since the systems with smaller n presented higher thermal stability than the free enzyme and glutaraldehyde immobilized GDH (MagNP-APTS/GDH and MagNP@SiO₂-APTS/GDH) cases.

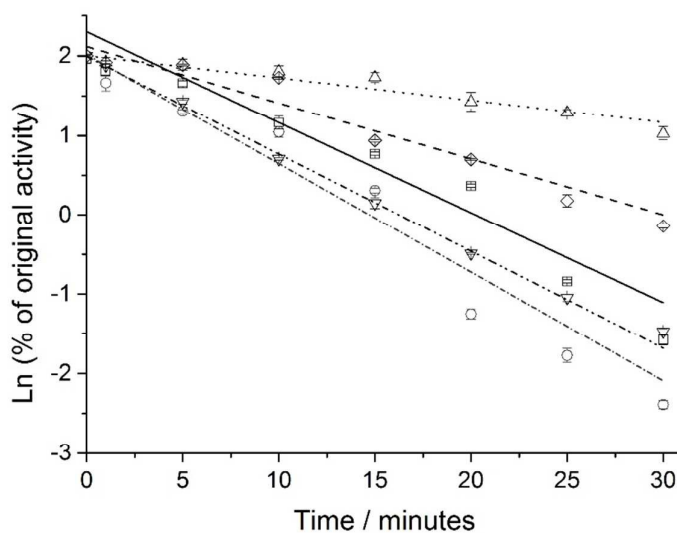


Figure 2. Enzyme inactivation at 50°C and pH 7.5. Free GDH (solid line, o), MagNP-APTS/GDH (\square), MagNP@SiO₂-APTS/GDH (∇), MagNP-APTS/Glyoxyl-Agarose/GDH (\triangle) and MagNP@CMC/GDH (\diamond).

In agreement with the ΔH^\ddagger values (Table 1), temperature-dependence catalysis for the immobilized systems presented a more constant dependence of pH vs activity, as can be seen in Figure 3. Free GDH (Figure 3, ∇) reaches 100 % of glutamate conversion at 32°C, while MagNP-APTS/GDH (Figure 3, \square) has its highest conversion (21%) at 25°C, which is also the optimum temperature for MagNP@SiO₂-APTS/GDH (Figure 3, \triangle), obtaining 30% of glutamate conversion. Immobilization of GDH through glyoxyl-agarose (Figure 3, o) presents a maximum conversion of 40% at 32°C, while MagNP@CMC/GDH (Figure 3, \diamond) has two apparent maximums, one at 25°C and the other at 47°C with conversions around 70%, which can be associated with a broad range of working temperature.

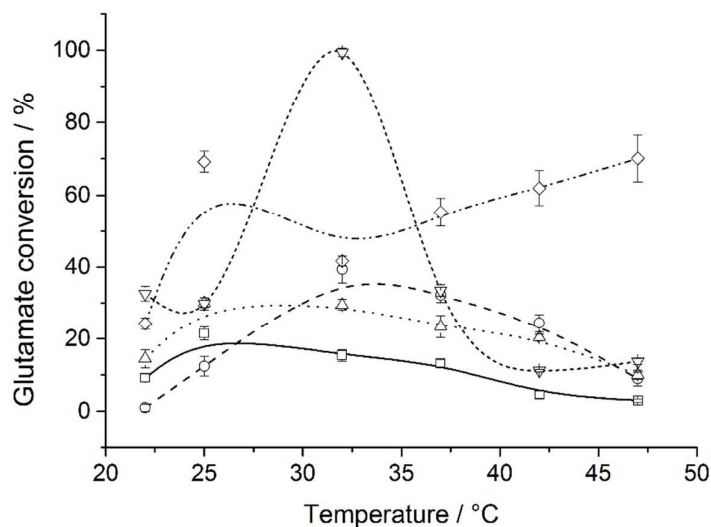


Figure 3. Influence of temperature at pH 7.5 on catalysis for free GDH (∇), MagNP-APTS/GDH (\square), MagNP@SiO₂-APTS/GDH (\triangle), MagNP-APTS/Glyoxyl-Agarose/GDH (o) and MagNP@CMC/GDH (\diamond).

Another feature displaying differences between the immobilized systems and free GDH was the catalytic behavior at different pHs, Fig. 4. An optimum pH at 8.8 was found for free GDH, with glutamate conversion around 30%, while MagNP@SiO₂-APTS/GDH and MagNP-APTS/Glyoxyl-Agarose/GDH had their optimum pHs at 7.5, with conversions of 25% and 12%,

respectively. This decrease in optimum pH was also observed by Petach *et al.*⁵⁴, who reasoned that the NH_4^+ ion does not diffuse away from the bond enzyme, therefore, the local environment around the immobilized enzyme seems more basic. A reduction of 0.8 unit in the optimum pH is observed for MagNP@CMC/GDH (Figure 4, \diamond) and surprisingly presents conversions around 70%, a value 2.5 times higher than free GDH. Remarkably, MagNP-APTS/GDH (Figure 4, \square) presents an increase in its catalytic activity with the increase of pH, reaching 18% of conversion at pH 9.8. An increase in the optimum pH was also observed by Barbotin *et al.*^{26a}, who also assumed an increase of pH in the $\text{NH}_4^+/\text{NH}_3$ equilibrium.

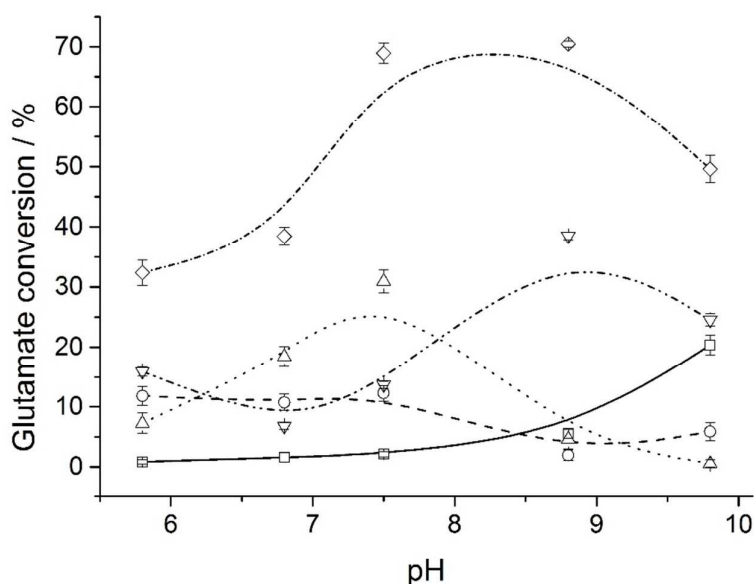


Figure 4. Influence of pH on catalysis at 25 °C for free GDH (∇), MagNP-APTS/GDH (\square), MagNP@SiO₂-APTS/GDH (\triangle), MagNP-APTS/Glyoxyl-Agarose/GDH (\circ) and MagNP@CMC/GDH (\diamond).

The greatest advantage of immobilized enzymes in contrast to free proteins, is their recyclability. Therefore, a study on the reuse of supported GDH was evaluated at the optimum pH and temperature for each system. MagNP-APTS/GDH and MagNP@SiO₂-APTS/GDH were active only during the first reaction cycle as can be seen in Figure 5, while MagNP@CMC/GDH although exhibiting the best performance in the first reaction cycle, showed a reduced activity after the second cycle and kept an average of 30% conversion up to the 10th cycle. The most stable system among the immobilization methods was MagNP-APTS/Glyoxyl-Agarose/GDH, demonstrating a nearly constant glutamate conversion activity around 40%, during the 10 monitored cycles.

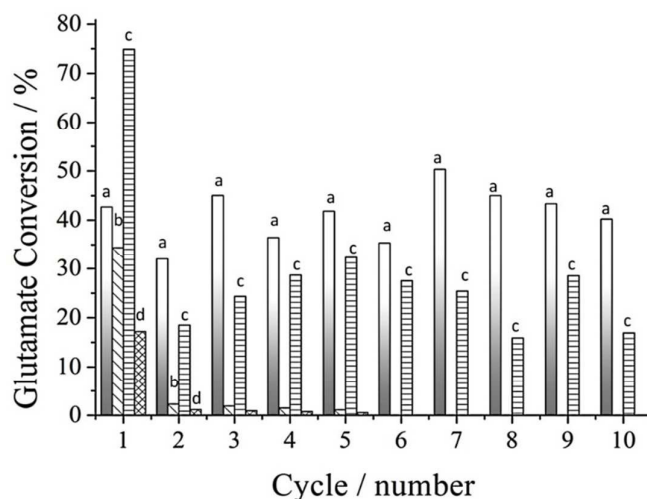


Figure 5. Recyclability of the immobilized systems: MagNP-APTS/Glyoxyl-Agarose/GDH (a); MagNP@SiO₂-APTS/GDH (b); MagNP@CMC/GDH (c) and MagNP-APTS/GDH (d).

For a deeper investigation on the immobilized GDH, topology and phase contrast images were obtained *via* Atomic Force Microscopy (AFM). In all the systems, after the drying process, a subsequent aggregation was observed with the application on mica, even under highly diluted conditions. This aggregation lead to the formation of clusters of variable sizes as shown in the typical topographic and phase contrast images in Figure 6. Better information can be taken from the phase contrast images, since mica and the magnetic nanoparticles are *hard* and anything displaying an opposite contrast can be considered as *soft*⁵⁵, as for example, the enzyme and agarose/cellulose. Therefore, in the phase contrast image for MagNP-APTS/GDH, MagNP-APTS/GlyoxylAgarose/GDH and MagNP@CMC/GDH (Figure 6 A, C and D-II), apparently, magnetic nanoparticles are anchored on organic aggregates. This situation is likely to be reversed in MagNP@SiO₂-APTS/GDH system, with the inclusion of magnetic particles in the aggregates, since almost no contrast is observed in Figure 6B-II.

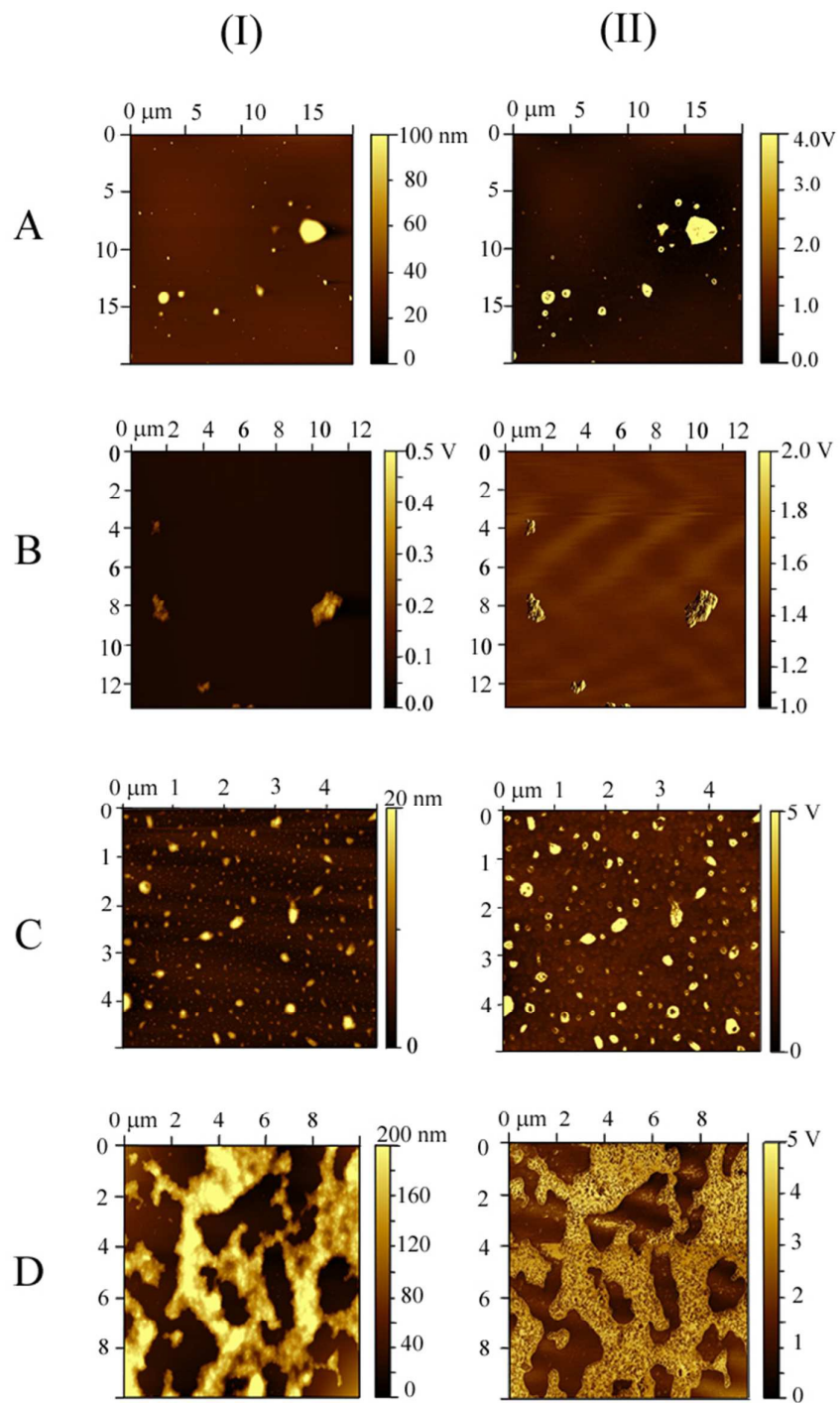


Figure 6. Atomic Force Microscopy images: (I) Topography, (II) Phase contrast for: (A) MagNP-APTS /GDH, (B) MagNP@SiO₂-APTS/GDH, (C) MagNP-APTS/Glyoxyl-Agarose/GDH and (D) MagNP@CMC/GDH.

Collectively, all these data indicate that conformational changes took place during the immobilization processes. Suggestion of 3D conformational changes of GDH are explicitly in MagNP-APTS/GDH as the less stable system, in MagNP@CMC/GDH as the most active system and in MagNP-APTS/Glyoxyl-Agarose/GDH as the most recyclable system. Therefore, other information are needed for a more comprehensive view of these systems.

In this regard, Raman spectroscopy is one of the most important tools for structural characterization of proteins.⁵⁶ Changes in the secondary and/or tertiary structure of proteins during a biochemical transformation⁵⁷ can be detected by the identification of specific bands associated with α -helix and β -sheet elements.⁵⁸ However, typically, the interpretation goes in the direction of the shapes of amide I and amide III bands.⁵⁹ In our case, free and immobilized GDH were submitted to a Confocal Raman Spectroscopy monitoring before and after glutamate and NAD^+ addition (Figure 7). According to such studies, it was evident that free GDH (Figure 7A) doesn't present spectroscopic changes with the addition of glutamate (Figure 7A, red line) and NAD^+ (Figure 7A, blue line), keeping the amide I band centered at 1634 cm^{-1} . The systems that resemble free GDH in this behavior are MagNP@SiO₂-APTS/GDH (Figure 7C) and MagNP-APTS/Glyoxyl-Agarose/GDH (Figure 7D) with the amide I band at 1634 and 1629 cm^{-1} , respectively. Also, MagNP@SiO₂-APTS/GDH and MagNP-APTS/Glyoxyl-Agarose/GDH didn't present spectroscopic changes upon the substrates addition.

The initial spectrum of MagNP-APTS/GDH (Figure 7B) has its amide I band maximum at 1633 cm^{-1} (black line, Figure 7B). When glutamate is added to this enzyme its amide I band maximum is blue shifted to 1662 cm^{-1} (red line, Figure 7B), with the rise of a small band at 1733 cm^{-1} , which indicates the presence of hydrophobic groups around a carboxyl that changes its position upon glutamate binding.⁶⁰ With the addition of NAD^+ (blue line, Figure 7B) amide I band red shifts to 1650 cm^{-1} .

The most distinct system is MagNP@CMC/GDH (Figure 7E) with an amide I band at 1660 cm^{-1} (black line, Figure 7E), corresponding to a decrease of intermolecular β structures, however, with the addition of glutamate these structures seem to have an increase in the contribution of intermolecular β structures, presenting a maximum at 1623 cm^{-1} .⁶¹ When NAD^+ is added, a band at 1733 cm^{-1} arises, indicating that the carbonyl of an aminoacid from the NAD^+ binding site is close to a hydrophobic site.⁶⁰

The emergence of the band at 1733 cm^{-1} can be further inspected, since it indicates an approximation between hydrophobic and carboxylic groups. Therefore, an examination of the 3D structure of bovine liver GDH structure (PDB code, 3MW9) with PyMol program, revealed

the residues K90, K126, K114 and R211 as the amino acids responsible for glutamate binding²³ and residues V255, E275, S276, Q330 and S327 responsible for NAD⁺ binding. Close to the carbonyl of E275 in NAD⁺ binding site there is a phenylalanine residue (F252), as can be seen in Figure 7, which could be the source of hydrophobic moiety in MagNP@CMC/GDH after NAD⁺ addition. The system MagNP-APTS/GDH has a similar band which only arises after glutamate addition. In the last case, carbonylic groups from R211 and K90 can approximate to Y382 and F122, respectively, after inclusion of glutamate in its binding site, due to their proximity (Figure 8) and possible change the active site conformation.

More importantly, unfolding can be observed in Confocal Raman Spectroscopy, by the sharpening of bands present in amide III region (1230-1300 cm⁻¹)^{58, 62}. The extended amide III region is meaningful since the coupling of N-H and C_α-H deformations is very sensitive to geometry and generates informative band structures.⁶³ In our experiments, GDH uncoiling is highly perceptible after glutamate addition in MagNP@CMC/GDH system (Figure 7 E2), with a noticeable increase of the bands in amide III region. This feature can be observed at a smaller extent in MagNP-APTS/Glyoxyl-Agarose/GDH, while the other systems have inconclusive amide III region. In MagNP@CMC/GDH system, a refolding is also readily observed after NAD⁺ addition, with the restitution of a similar spectra of the one prior to the substrates addition (Figure 7 E3).

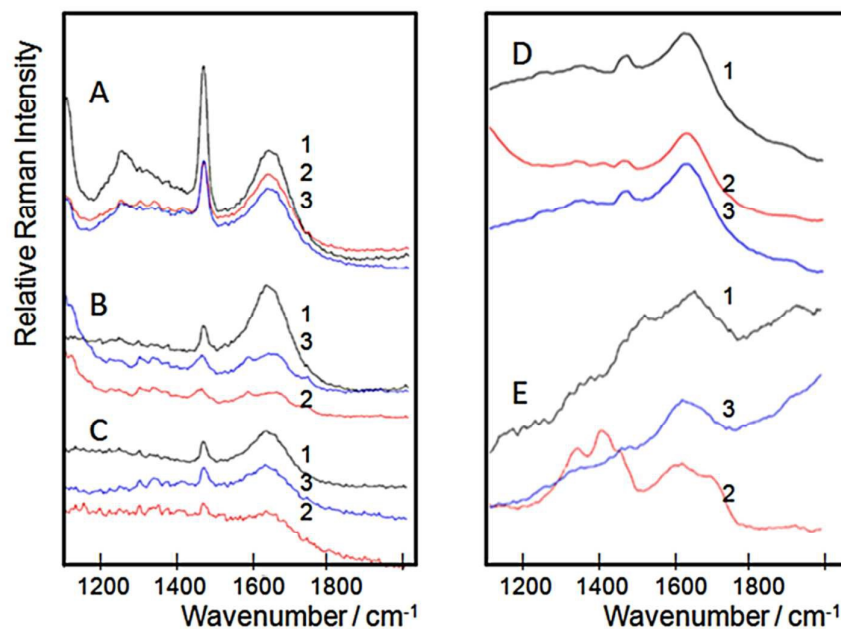


Figure 7. Confocal Raman Spectra for (A) free GDH, (B) MagNP-APTS/GDH, (C) MagNP@SiO₂-APTS/GDH, (D) MagNP-APTS/Glyoxyl-Agarose/GDH, (E) MagNP@CMC/GDH before (black line, 1) and after glutamate addition (red line, 2) and NAD⁺ addition (blue line, 3).

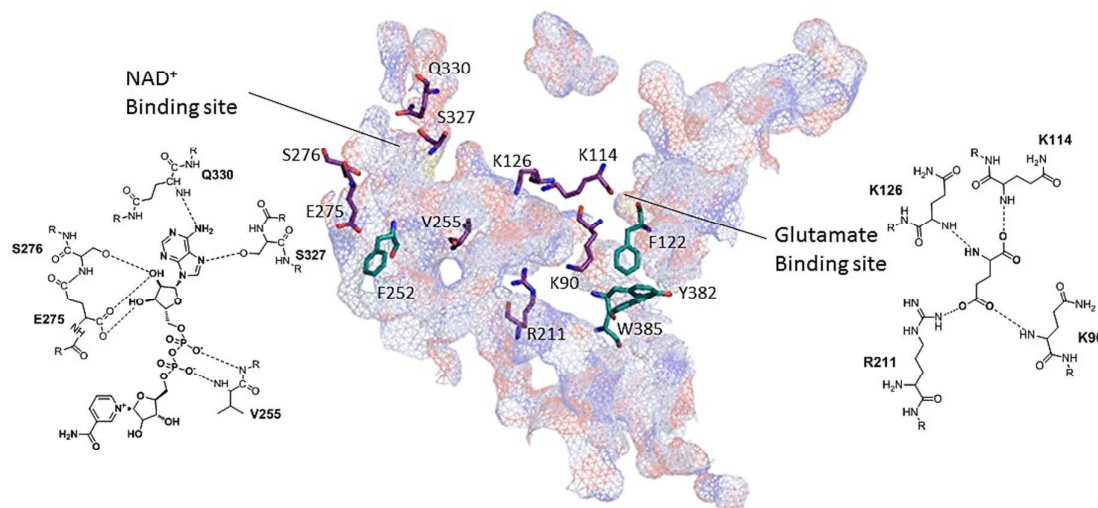


Figure 8. Representation of the NAD⁺ and glutamate binding sites in GDH. Residues in purple are responsible for substrate binding. Residues in turquoise possess an aromatic moiety capable of interacting to carbonyls from the active sites.

Allegedly, it is expected to observe different allosteric responses in immobilized GDH, since GDH allostery demand subunits to interact and sense each other^{26c}, and upon immobilization, different 3D conformations were achieved, as were evidenced by Raman spectra (Figure 6). The antenna from GDH is engaged in the allostery,⁶⁴ since the closure of one subunit requires a distortion at the back portion of the antenna^{65 23}. For example, the inhibition through GTP requires an antenna deformation while GDH closes.^{65 23} In our experiments, increasing concentrations of the allosteric regulators, ADP, GTP and ATP⁶⁶ were evaluated by comparison of the initial reaction rates (Tables 2, 3 and 4, respectively). Increasing concentrations of ADP, activated all the immobilized GDH but MagNP-APTS/GDH, which exhibited a slight inhibition, as evidenced by the decay of V_{initial} (Table 2, entry 2).

Table 2. Initial reaction rates of free and supported GDH at increasing concentrations of ADP.

Entry	System	Initial Reaction Rates, V_{initial} ($\text{mol L}^{-1} \text{s}^{-1}$)			
		0 μM ADP	10 μM ADP	50 μM ADP	100 μM ADP
1	Free GDH	1,5x10 ⁻⁷ ($\pm 9 \times 10^{-8}$)	2,2x10 ⁻⁷ ($\pm 6 \times 10^{-8}$)	2,2x10 ⁻⁷ ($\pm 2 \times 10^{-8}$)	2,1x10 ⁻⁷ ($\pm 3 \times 10^{-8}$)
2	MagNP-APTS/GDH	6,9 x10 ⁻⁸ ($\pm 3 \times 10^{-8}$)	6,3 x10 ⁻⁸ ($\pm 3 \times 10^{-8}$)	5,4 x10 ⁻⁸ ($\pm 1 \times 10^{-8}$)	4,3 x10 ⁻⁸ ($\pm 1 \times 10^{-8}$)
3	MagNP@SiO ₂ - APTS/GDH	3,9x10 ⁻⁸ ($\pm 9 \times 10^{-9}$)	4,9 x10 ⁻⁸ ($\pm 2 \times 10^{-8}$)	1,5 x10 ⁻⁷ ($\pm 2 \times 10^{-8}$)	2,5 x10 ⁻⁷ ($\pm 6 \times 10^{-8}$)
4	MagNP-APTS/Glyoxyl- Agarose/GDH	1,1x10 ⁻⁷ ($\pm 5 \times 10^{-8}$)	1,0 x10 ⁻⁷ ($\pm 3 \times 10^{-8}$)	1,8 x10 ⁻⁷ ($\pm 4 \times 10^{-8}$)	2,8 x10 ⁻⁷ ($\pm 2 \times 10^{-7}$)
5	MagNP@CMC/GDH	5,7x10 ⁻⁸ ($\pm 3 \times 10^{-8}$)	3,3 x10 ⁻⁷ ($\pm 2 \times 10^{-7}$)	6,8 x10 ⁻⁷ ($\pm 1 \times 10^{-7}$)	8,2 x10 ⁻⁷ ($\pm 1 \times 10^{-7}$)

Glutamate dehydrogenase natural inhibitor, GTP,⁶⁷ only inhibited free GDH and MagNP@CMC/GDH (Table 3, entries 1 and 5). The systems MagNP-APTS/Glyoxyl-Agarose/GDH and MagNP@SiO₂-APTS/GDH essentially weren't affected by increasing concentrations of GTP (Table 3, entries 3 and 4). Curiously, MagNP-APTS/GDH exhibited activation upon increasing GTP concentrations (Table 3, entry 2).

Table 3. Initial reaction rates of free and supported GDH at increasing concentrations of GTP.

Entry	System	Initial Reaction Rates (V_{initial} ($\text{molL}^{-1} \text{s}^{-1}$))			
		0 μM GTP	10 μM GTP	50 μM GTP	100 μM GTP
1	Free GDH	6,4x10 ⁻⁷ ($\pm 2 \times 10^{-8}$)	4,2x10 ⁻⁷ ($\pm 5 \times 10^{-8}$)	9,2x10 ⁻⁸ ($\pm 7 \times 10^{-8}$)	4,4x10 ⁻⁸ ($\pm 1 \times 10^{-8}$)
2	MagNP-APTS/GDH	8,3 x10 ⁻⁹ ($\pm 1 \times 10^{-9}$)	3,8 x10 ⁻⁸ ($\pm 2 \times 10^{-9}$)	5,34 x10 ⁻⁸ ($\pm 1 \times 10^{-9}$)	8,7 x10 ⁻⁸ ($\pm 7 \times 10^{-9}$)
3	MagNP@SiO ₂ - APTS/GDH	1,8x10 ⁻⁷ ($\pm 4 \times 10^{-8}$)	1,3x10 ⁻⁷ ($\pm 2 \times 10^{-8}$)	1,6x10 ⁻⁷ ($\pm 2 \times 10^{-8}$)	1,2x10 ⁻⁷ ($\pm 4 \times 10^{-8}$)
4	MagNP-APTS/Glyoxyl- Agarose/GDH	6,0x10 ⁻⁸ ($\pm 2 \times 10^{-8}$)	5,26x10 ⁻⁸ ($\pm 9 \times 10^{-9}$)	9,2x10 ⁻⁸ ($\pm 2 \times 10^{-8}$)	7,3x10 ⁻⁸ ($\pm 6 \times 10^{-9}$)
5	MagNP@CMC/GDH	4,7x10 ⁻⁷ ($\pm 1 \times 10^{-7}$)	2,4x10 ⁻⁷ ($\pm 9 \times 10^{-8}$)	1,17x10 ⁻⁷ ($\pm 1 \times 10^{-8}$)	1,8x10 ⁻⁷ ($\pm 2 \times 10^{-8}$)

Due to the difference in allosteric response to ADP and GTP, and lack of information whether adenine or triphosphate moiety were the responsible moieties for the distinct responses, increasing concentrations of ATP were also evaluated. The ATP- based allostereism is

more complex than ADP and GTP ones⁶⁸, since it inhibits glutamate dehydrogenase at low (1-100 $\mu\text{mol L}^{-1}$) and high (1-10 mmol L^{-1}) concentrations due to binding at the GTP site, but at intermediate concentrations (100 $\mu\text{mol L}^{-1}$ to 1 mmol L^{-1}) it becomes an activating agent as it binds to the ADP site.^{64,69} Consequently, it would be expected that systems with ADP-activation behavior, to be activated when intermediate concentrations (100 $\mu\text{mol L}^{-1}$ to 1 mmol L^{-1}) of ATP and *vice versa*. From the immobilized GDH systems, consistently, MagNP-APTS/GDH shows the most unusual behavior, being inhibited at 100 μM of ATP, while at higher concentrations of ATP, it did not exhibit allostereism (Table 4, entry 2). The other systems, in higher or minor magnitudes, exhibited a similar behavior to free GDH.

Table 4. Initial reaction rates of free and supported GDH at increasing concentrations of ATP.

Entry	System	Initial Reaction Rates (V_{initial} ($\text{molL}^{-1}\text{s}^{-1}$))				
		0 μM ATP	100 μM ATP	1mM ATP	10mM ATP	100mM ATP
1	Free GDH	$9,8 \times 10^{-8}$ ($\pm 2 \times 10^{-8}$)	$1,1 \times 10^{-7}$ ($\pm 1 \times 10^{-8}$)	$1,6 \times 10^{-7}$ ($\pm 2 \times 10^{-8}$)	$9,0 \times 10^{-8}$ ($\pm 2 \times 10^{-8}$)	$1,6 \times 10^{-8}$ ($\pm 2 \times 10^{-8}$)
2	MagNP-APTS/GDH	$2,8 \times 10^{-8}$ ($\pm 1 \times 10^{-8}$)	$3,4 \times 10^{-8}$ ($\pm 1 \times 10^{-8}$)	$1,2 \times 10^{-8}$ ($\pm 1 \times 10^{-8}$)	$2,4 \times 10^{-8}$ ($\pm 1 \times 10^{-8}$)	$2,8 \times 10^{-8}$ ($\pm 2 \times 10^{-8}$)
3	MagNP@SiO ₂ -APTS/GDH	$4,4 \times 10^{-8}$ ($\pm 1 \times 10^{-8}$)	$5,7 \times 10^{-8}$ ($\pm 8 \times 10^{-9}$)	$6,0 \times 10^{-8}$ ($\pm 2 \times 10^{-9}$)	$7,9 \times 10^{-10}$ ($\pm 7 \times 10^{-10}$)	$3,5 \times 10^{-8}$ ($\pm 2 \times 10^{-8}$)
4	MagNP-APTS/Glyoxyl- Agarose/GDH	$1,6 \times 10^{-8}$ ($\pm 2 \times 10^{-8}$)	$2,4 \times 10^{-8}$ ($\pm 7 \times 10^{-9}$)	$2,9 \times 10^{-8}$ ($\pm 3 \times 10^{-9}$)	$7,9 \times 10^{-9}$ ($\pm 7 \times 10^{-9}$)	$3,8 \times 10^{-9}$ ($\pm 3 \times 10^{-9}$)
5	MagNP@CMC/GDH	$3,16 \times 10^{-8}$ ($\pm 1 \times 10^{-8}$)	$1,0 \times 10^{-7}$ ($\pm 9 \times 10^{-8}$)	$1,3 \times 10^{-7}$ ($\pm 8 \times 10^{-8}$)	$2,4 \times 10^{-9}$ ($\pm 1 \times 10^{-9}$)	$3,1 \times 10^{-9}$ ($\pm 2 \times 10^{-8}$)

In support to the allosteric kinetics, enzyme digestion studies using trypsin were carried out and the fragments were analyzed by MALDI-TOF. A careful analysis of the fragments was performed in accordance to the amino acid sequence of GDH in a similar manner to Wacker *et al.*⁷⁰ aiming the evaluation of sites blockage and any possible conformational change of GDH upon immobilization to magnetic supports. The enzymatic digestion was carried out in the presence and absence of the allosteric molecules.

The most intense peaks observed in these digestion experiments are highlighted in Figure 9. Essentially, 10 main fragments are obtained: 1-11, 450-469, 291-305, 12-19, 28-33, 9-40, 156-174, 137-154 and 476-501, which showed to be characteristic of the enzyme motion after addition of ADP or GTP. For instance, in the case of free GDH in the absence of ADP and

GTP the main fragment is composed by the amino acids sequence 1-11 (m/z 1353), followed by the fragment 450-469 (m/z 2311) and 291-305 (m/z 1714). In the presence of ADP and GTP, the fragment 1-11 remains the major one, however in smaller extent. Exposure of the fragments 12-19 (m/z 100) and 28-33 (m/z 715) is detected when GDH is in presence of GTP. Both fragments (12-19 and 28-33) are directly opposite to the GTP site (Figure 8, yellow line), indicating the enzyme conformation change upon GTP binding. On the other hand, ADP increases the preferential digestion of the fragment 450-469, which is opposite to its binding site.

It is expected therefore, to observe similar patterns of digestion when inhibition or activation is observed, independently of the regulator used. This assumption was proved to be correct, since MagNP-APTS/GDH when in presence of its inhibitor, ADP, presented the fragment 12-19, which is characteristic of GTP binding to free GDH. This fragment is also observed in MagNP@SiO₂-APTS/GDH without allosteric regulators and in MagNP-APTS-GlyoxylAgarose/GDH in the presence of both GTP and ADP. Another important fragment to be highlighted is fragment 156-174, which is only observed for MagNP@SiO₂-APTS/GDH and MagNP-APTS-GlyoxylAgarose/GDH when in presence of GTP, which suggests an antenna torsion and possible blockage of GTP site. The fragment 476-501, seen in MagNP@SiO₂-APTS/GDH, is associated with an internal conformation of free GDH and occurs both in presence of ADP and GTP, thus, possibly, a partial protein unfolding occurs to expose internal structures of GDH after the addition of allosteric regulators for MagNP@SiO₂-APTS/GDH.

MagNP@CMC/GDH is perhaps the most similar system to free GDH, since fragments 1-11, 291-305 and 450-469 are favored in the digestion experiments. The addition of ADP to this system, permits a preferential fragmentation of 137-154, which would indicate an exposure of the internal parts that connects the subunits.

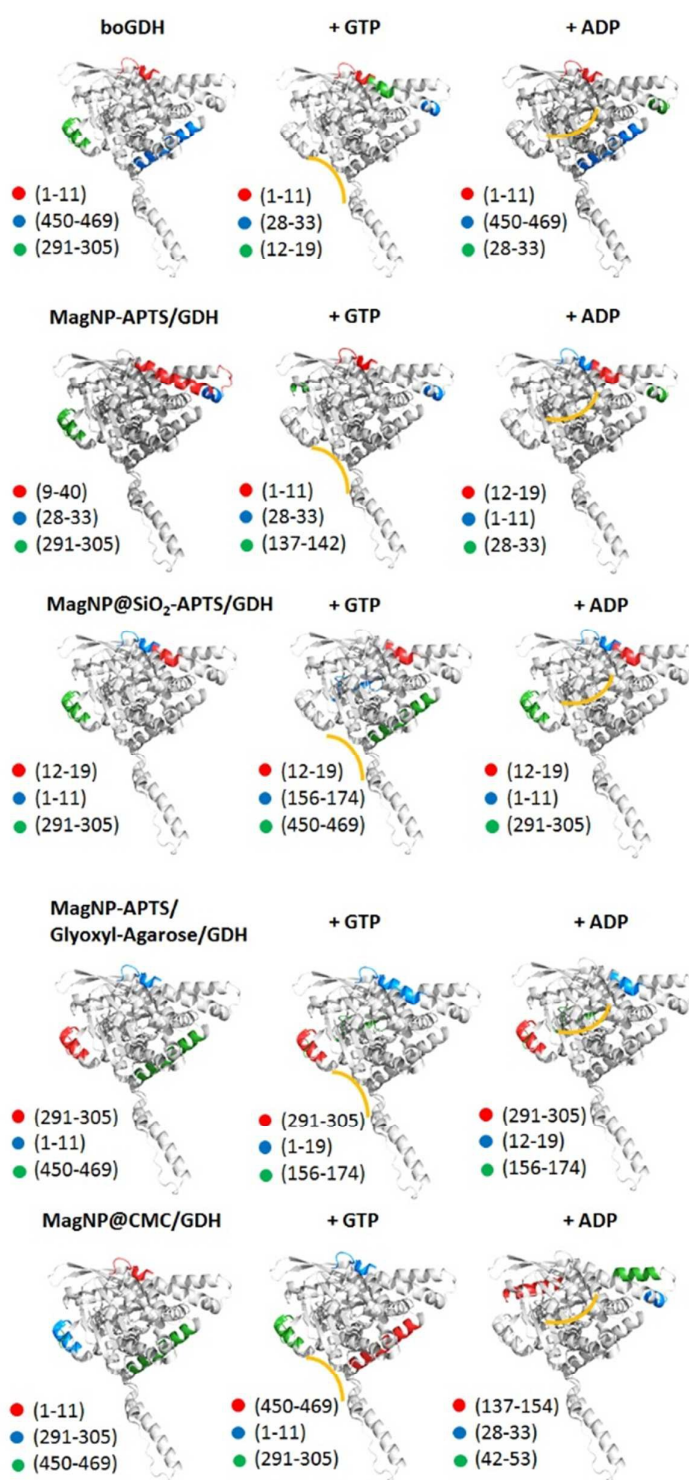


Figure 9. Main fragments in a monomer that are obtained in the tryptic digestion before and after the addition of ADP and GTP. In red, blue and green are the main, second and third most abundant fragments, respectively. In yellow is the indication of the ADP and GTP binding sites.

Discussion

The obtained results corroborate to a conclusion that each magnetic support is influencing to a certain extent the final 3D structure from glutamate dehydrogenase. For instance, glutaraldehyde-based immobilization gives less stable enzymatic systems (Figure 1, supports A and B), while larger aldehyde cross-coupling results in higher stability of GDH (Figure 1, supports C and D), in agreement to other reported studies⁷¹⁻⁷⁴. This singularity is also pronounced in the allosteric-response experiments, with ADP activation of all immobilized systems but MagNP-APTS/GDH. In addition, GDH inhibition occurs in free GDH and MagNP@CMC/GDH, though in MagNP-APTS/GDH, GTP actually acts as an activator, and in the other systems, MagNP-APTS/Glyoxyl-Agarose/GDH and MagNP@SiO₂-APTS/GDH, GTP doesn't have a marked influence in their catalysis. Even more surprisingly are the results with ATP, because MagNP-APTS/GDH is inhibited at activating concentrations, while the other systems had similar activity to free GDH.

A classical argument on allostery is around the influence of conformational changes between two well-defined structures, with protein flexibility playing an essential role.⁷⁵ In glutamate dehydrogenase for example, it is said that GTP preferentially binds *via* the phosphates to Iso216 and Ser217 to the open form of GDH⁷⁶, while ADP binds *via* adenosine to Arg463 in an hydrophobic site of both forms of GDH, apo and holo⁷⁶. However, allosteric behavior is not exclusive of highly ordered enzymes, since even disordered proteins⁷⁵ and proteins with no conformational change⁷⁷ display this behavior, meaning that there is an entropic contribution to allostery.⁷⁵ In account to entropic contributions, are the works describing environmental conditions that change the cooperativity between subunits which transform an activator into a repressor, or vice-versa. This theory is called intrinsic disorder mechanism^{19a}. The first description of this theory was reported by Cooper and Dryden⁷⁷, who guide to the dynamics of proteins and consider that intramolecular motions (hinge-bending, breathing, local unfolding, among others) influence the overall allostery. For instance, local unfolding has been shown to give thermodynamic stability due to the reduction of a protein's domain flexibility and result in allosteric response.⁷⁸ In addition, it is known that increase in binding affinity can be due to local unfolding, enhancing protein's conformational flexibility.⁷⁹

80

As a consequence from these relationships between intramolecular motions and allostery we might develop a theory behind the anomaly in our GDH immobilized systems. In this study, the lowest $S_{0.5}$ is observed in MagNP@CMC/GDH (Table 1), implying the highest substrate affinity among all GDH used and consequently, a higher protein flexibility. The

elasticity of GDH on MagNP@CMC leads to a larger globally extended conformation since it should accompany the reduction in binding affinity. As could be observed in Raman spectroscopy (Figure 7 E), GDH supported on MagNP@CMC uncoiled after glutamate addition and this local unfolding was less evident in MagNP-APTS/Glyoxyl-Agarose/GDH and MagNP@SiO₂-APTS/GDH (Figure 7 C and D), which present the second lowest $S_{0.5}$ (Table 1). Without changing a protein's conformation, Petit *et al.*⁸¹ observed a reduced binding affinity when a α -helix was removed from a protein. In our case, it is believed that MagNP-APTS is bonded on the GDH's antenna (allosteric response experiments: Tables 2, 3 and 4 and trypsin digestion), and precisely MagNP-APTS/GDH, is the system with a diminished substrate binding affinity. Comparing MagNP-APTS/GDH behavior to Petit *et al.*⁸¹ study, the almost 2 fold increase in $S_{0.5}$ for MagNP-APTS/GDH can be attributed to an entropic nature of glutamate binding which can be also related to its peculiar allosteric response.⁸²

In another study, tethering a protein through a α -helix produced a more thermal-stable protein than when the attachment was through a flexible loop⁸³. From this finding it is expected that MagNP-APTS/GDH to be tethered through a loop since it is the least thermal stable system. A careful analysis of GDH antenna indicates that 27% of the more exposed loops are concentrated in the antenna region, therefore, due to the fact that MagNP-APTS/GDH is the least thermal stable system and has the most abnormal allosteric response, it would indicate a higher probability of GDH immobilization on MagNP-APTS *via* the loop of the antenna. Following this reasoning, MagNP@SiO₂-APTS/GDH should also be immobilizing GDH through a loop, since it is the second least thermal-stable system. The tryptic digestion and allosteric-response experiments suggest that GTP binding site is possibly blocked, suggesting that MagNP@SiO₂-APTS is most probably bonded to GTP site. From the 3D structure from GDH, there is an indication that 36% of the exposed loops are next to GTP binding site, which corroborates to our assumption of immobilization next to the GTP binding site.

However, the conjecture of possible conformational states that are favorably immobilized should accompany the other behaviors of the immobilized systems, such as for example, the allosteric response experiments. To answer whether GDH allosterism is largely dependent on entropy issues more than on enthalpy ones, the relative stability of all the possible states should be addressed.^{75,84} Here, to determine the most probable states present in the immobilized systems, a comparison between fragments from free GDH and immobilized GDH was performed. After the determination of states with higher probability of occurring, the local folding/unfolding of these states was assumed according to Hilser *et al.*^{19a} method (Supplementary Material).

First of all, free GDH is assumed to bear 8 possible states for each monomer as shown in Figure 10. Hence, the homohexameric structure would have 36 possible states, but for sake of simplification, we are assuming just one monomer. The next step is to determine whether a molecule is activating or inactivating, which would mean a positive or negative ΔG_{int} (difference of the free energy of unfolding each domain and the energy of breaking the interactions between domains), for activator and inhibitor molecules, respectively. Therefore, upon ADP addition, the domain responsible for ADP binding will be preferentially stabilized and states 1,2,3 and 4 (Figure 10) will possess a higher probability in the ensemble. Since ADP is an activator of GDH, ΔG_{int} has a positive value, meaning that domains from ADP and glutamate binding are positively coupled. The positive coupling indicates that breaking the interaction between ADP and glutamate sites will be unfavorable, consequently, after addition of glutamate and NAD^+ , a stabilization of glutamate binding site occurs, increasing the probability of finding states 1 and 3 in the ensemble (as shown in Figure 10). For GTP interaction, an opposite effect is observed, since ΔG_{int} has a negative value (interaction between GTP and glutamate binding sites) and the unfolded states dominate the ensemble probabilities (states 1,2,6 and 7). Comparing the addition of allosteric regulators with an ensemble without regulators (preferential states 1,2,5 and 6) it is clear that ADP addition increases the probability of active GDH in solution, while GTP decreases this probability, demonstrating this effect in the total enzyme activity.

To illustrate this methodology in an immobilized GDH, we have chosen $\text{MagNP@SiO}_2\text{-APTS/GDH}$ system, since its visualization is straightforward. Fragmentation of this system indicate the existence of fragment 12-19 in the presence and absence of the allosteric regulators ADP and GTP. This fragment suggest the major probability of conformations where GTP site is folded, as shown in Figure 10 (states 1, 2, 6 and 7). ADP addition increases the probability of states 1 and 2, while GTP addition has no influence on the ensemble probability as can be seen in Figure 10. This result corroborate to the experimental data obtained, with GTP not acting as an inhibitor for $\text{MagNP@SiO}_2\text{-APTS/GDH}$ system.

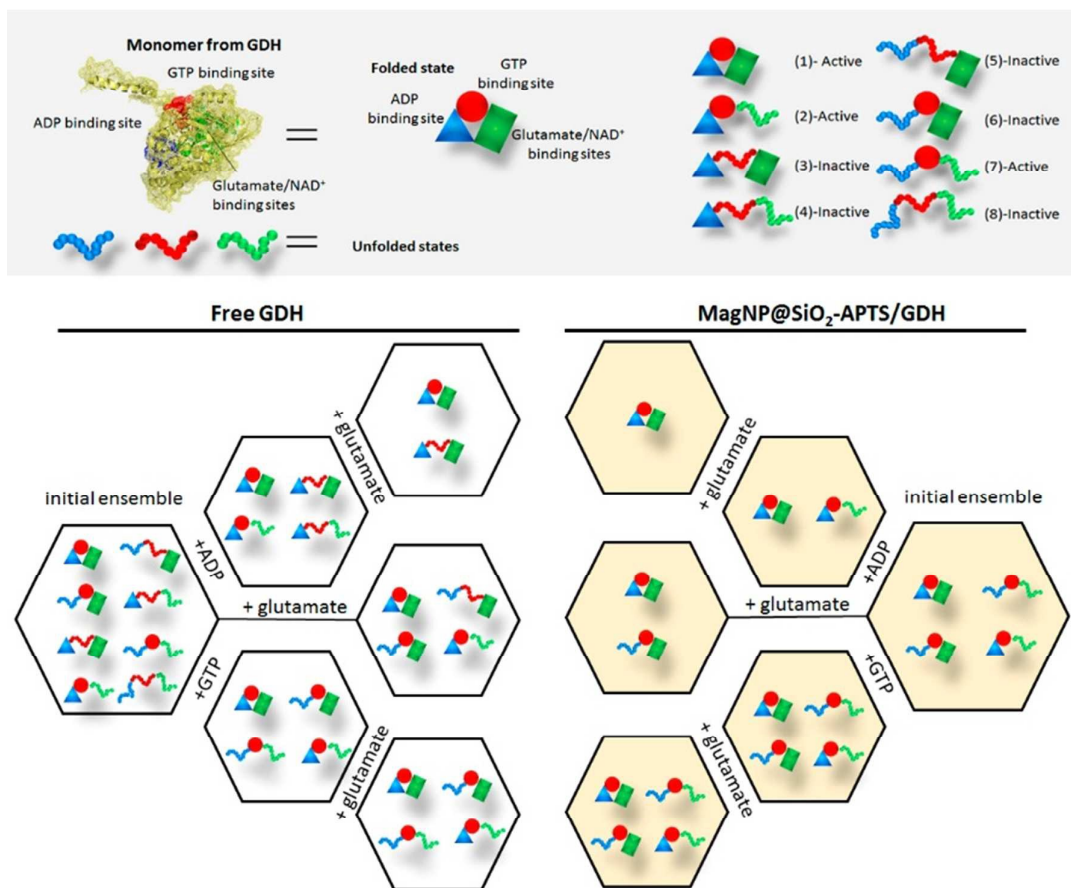


Figure 10. Representation of GDH monomer conformation ensemble for free GDH (white hexagons) and MagNP@SiO₂-APTS/GDH (pink hexagons). The highest probability states are shown in the hexagons, while all the other states are present in lower probabilities.

The same reasoning can be used for the other 3 immobilized systems, as can be seen in the supplementary material. Briefly, MagNP-APTS/GDH possibly presents as major conformations in the initial ensemble the unfolded glutamate and NAD⁺ binding site, which would also explain the higher $S_{0.5}$ for this system. This statement can be reasoned by the trypsin digestion experiments and by Raman spectroscopy, in which, the later indicates a folding of the glutamate binding site after addition of glutamate (amide I band shift from 1633 to 1662 cm⁻¹). The increase in optimum pH can be also reasoned by the conformational change, since pK_a of K126 increases in 1 unit of pH (from 8.8 to 9.8), shifting to a pK_a of an exposed lysine (≈ 10.3), which agrees with the higher percentage of unfolded states in the initial ensemble. More importantly, one can highlight the difference on immobilization and obtained dynamics for systems MagNP-APTS/GDH and MagNP@SiO₂-APTS/GDH, since their

difference is only on the iron exposure to the surface. MagNP-APTS/GDH have as an initial ensemble, a higher probability of unfolded states (high $S_{0.5}$), which may be due to iron coordination and interaction to the enzyme residues, while MagNP@SiO₂-APTS/GDH would have a silica shell preventing this interaction, but the immobilized preferential conformation using the silica-shell magnetite is in the inactive form, which explains the lower K_{cat} for MagNP@SiO₂-APTS/GDH (0,19 s⁻¹) than for MagNP-APTS/GDH (0,27 s⁻¹).

The pK_a of K126 in MagNP@SiO₂-APTS/GDH and MagNP-APTS/Glyoxyl-Agarose/GDH is also modified ($pK_a \approx 7.5$). However, their Raman spectra is very similar to free GDH's one and the argument behind the different catalysis are based on the tryptic digestion and the initial ensemble states. Differently from MagNP@SiO₂-APTS/GDH, system MagNP-APTS/Glyoxyl-Agarose/GDH exhibits as most probable states the completely folded one and the ADP unfolded one. The first state is active and the second one is inactive and since GDH has the glutamate-site most probably immobilized in the folded conformation, the higher recoverability of this system could be explained as the favoring of active and folded conformational states. Another system that presents a folded preference of glutamate binding site is MagNP@CMC/GDH, but in that case, 75% of the states are active, therefore, the higher activity (2.5 time higher than free GDH) exhibited for this system is explained as the immobilization of preferential active states.

As a conclusion of this theory, the immobilization of GDH on different magnetic supports resulted in distinct enzymatic activities majorly due to the stabilization of different dynamic-conformational states, which is a result of the system's entropy. The only system that actually behaves abnormally is MagNP-APTS/GDH, and this deviation is possibly due a negative ΔG_{int} energy between ADP and glutamate binding sites, while a positive ΔG_{int} is observed between GTP and glutamate binding sites, resulting in ADP/ATP ([ATP]= 100 $\mu\text{mol L}^{-1}$ - 1 mmol L⁻¹) inhibition and GTP/ATP ([ATP]=1-100 $\mu\text{mol L}^{-1}$ and 1-10 mmol L⁻¹) activation.

Conclusion

Upon immobilization on four different magnetic supports, glutamate dehydrogenase presented unusual catalytic behavior. The highly active MagNP@CMC/GDH was shown to be not as stable as MagNP-APTS/Glyoxyl-Agarose/GDH, while MagNP-APTS/GDH presented opposite allosteric responses. The intrinsic disorder mechanism was used to understand these behaviors, bringing explanations on the probability of each system to be active or inactive with ADP and GTP additions. MagNP@SiO₂-APTS/GDH was majorly immobilized on its inactive

conformation, therefore, clarifying the reason behind the null effect observed in MagNP@SiO₂-APTS/GDH catalysis after GTP addition. On the other hand, the highest activity of system MagNP@CMC/GDH can be explained by the existence of active major conformations, than in the free enzyme. In conclusion, the intrinsic disorder mechanism proved to be an important tool for understanding immobilized enzymes and the influence of the support on the protein total ensemble.

Acknowledgements

The support from FAPESP Grant 2008/10177-7 (Fundação de Amparo à Pesquisa do Estado de São Paulo) and CNPq (Conselho Nacional de Desenvolvimento Científico e Tecnológico) are gratefully acknowledged.

References

1. Mateo, C.; Palomo, J. M.; Fernandez-Lorente, G.; Guisan, J. M.; Fernandez-Lafuente, R., Improvement of enzyme activity, stability and selectivity via immobilization techniques. *Enzyme and Microbial Technology* **2007**, *40* (6), 1451–1463.
2. Sheldon, R. A., Enzyme Immobilization: The Quest for Optimum Performance. *Adv. Synth. Catal.* **2007**, *349*, 1289.
3. (a) Secundo, F., Conformational changes of enzymes upon immobilisation. *Chem. Soc. Rev.* **2013**, *46*, 6250; (b) Santos, J. C. S. D.; Barbosa, O.; Ortiz, C.; Berenguer-Murcia, A.; Rodrigues, R. C.; Fernandez-Lafuente, R., Importance of the support properties for immobilization or purification of enzymes. *ChemCatChem* **2015**, *7* (16), 2413.
4. Netto, C. G. C. M.; Toma, H. E.; Andrade, L. H., Superparamagnetic nanoparticles as versatile carriers and supporting materials for enzymes. *Journal of Molecular Catalysis B: Enzymatic* **2013**, *85-86*, 71–92.
5. Brena, B. M.; Batista-Viera, F., Immobilization of Enzymes. In *Immobilization of Enzymes and Cells*, 2nd ed.; Guisán, J. M., Ed. Humana Press Inc.: Totowa, NJ, 2006.
6. *Heterogeneous Catalysis for Today's Challenges: Synthesis, Characterization and Applications*. The Royal Society of Chemistry: Cambridge, UK, 2015.
7. Kingsley, L. J.; Lill, M. A., Substrate tunnels in enzymes: Structure–function relationships and computational methodology. *Proteins: Structure, Function and Bioinformatics* **2015**, *83* (4), 599.
8. (a) Rodrigues, R. C.; Ortiz, C.; Berenguer-Murcia, Á.; Torres, R.; Fernández-Lafuente, R., Modifying enzyme activity and selectivity by immobilization. *Chem. Soc. Rev.* **2013**, *42*, 6290; (b) Hanefeld, U.; Cao, L.; Magner, E., Enzyme immobilization: fundamentals and application. *Chem. Soc. Rev.* **2013**, *42* (15), 6211; (c) Clark, D. S., Can immobilization be exploited to modify enzyme activity? *TIBTECH* **1994**, *12*, 439.
9. Singh, R. K.; Tiwari, M. K.; Singh, R.; Lee, J.-K., From Protein Engineering to Immobilization: Promising Strategies for the Upgrade of Industrial Enzymes *Int. J. Mol. Sci.* **2013**, *14*, 1232.

10. Fernandez-Lafuente, R., Stabilization of Multimeric Enzymes: Strategies to prevent subunit dissociation. *Enzyme and Microbial Technology* **2009**, *45* (6-7), 405.
11. (a) Pedroche, J.; Yust, M. d. M.; Mateo, C.; Fernández-Lafuente, R.; Girón-Calle, J.; Alaiz, M.; Vioque, J.; Guisán, J. M.; Millána, F., Effect of the support and experimental conditions in the intensity of the multipoint covalent attachment of proteins on glyoxyl-agarose supports: Correlation between enzyme-support linkages and thermal stability. *Enzyme and Microbial Technology* **2007**, *40* (5), 1160; (b) Bezerra, C. S.; Lemos, C. M. G. d. F.; Sousa, M. d.; Gonçalves, L. R. B., Enzyme immobilization onto renewable polymeric matrixes: Past, present, and future trends. *Journal of Applied Polymer Science* **2015**, *132* (26).
12. (a) Garcia-Galan, C.; Barbosa, O.; Fernandez-Lafuente, R., Stabilization of the hexameric glutamate dehydrogenase from *Escherichia coli* by cations and polyethyleneimine. *Enzyme and Microbial Technology* **2013**, *52*, 211–217; (b) Bolivar, J. M.; Mateo, C.; Grazu, V.; Carrascosa, A. V.; Pessela, B. C.; Guisan, J. M., Heterofunctional supports for the one-step purification, immobilization and stabilization of large multimeric enzymes: Amino-glyoxyl versus amino-epoxy supports. *Process Biochemistry* **2010**, *45*, 1692–1698.
13. Wong, S. S.; Wong, L.-J. C., Chemical crosslinking and the stabilization of proteins and enzymes *Enzyme Microb. Technol.* **1992**, *14*, 866.
14. (a) Lencki, R. W.; Arul, J.; Neufeld, R. J., Effect of Subunit Dissociation, Denaturation, Aggregation, Coagulation, and Decomposition on Enzyme Inactivation Kinetics: II. Biphasic and Grace Period Behavior. *Biotechnology and Bioengineering* **1992**, *40*, 1427; (b) Poltorak, O. M.; Chukhray, E. S.; Torshin, I. Y., Dissociative thermal inactivation, stability, and activity of oligomeric enzymes. *Biochemistry (Mosc.)* **1998**, *63* (3), 303.
15. Jia, F.; Narasimhan, B.; Mallapragada, S., Materials-based strategies for multi-enzyme immobilization and co-localization: A review. *Biotechnology and Bioengineering* **2014**, *111* (2), 209.
16. Costa, J. P. d.; Oliveira-Silva, R.; Daniel-da-Silva, A. L.; Vitorino, R., Bionanoconjugation for Proteomics applications — An overview. *Biotechnology Advances* **2014**, *32* (5), 952.
17. Ding, S.; Cargill, A. A.; Medintz, I. L.; Claussen, J. C., Increasing the activity of immobilized enzymes with nanoparticle conjugation. *Current Opinion in Biotechnology* **2015**, *34*, 242.
18. Palomo, J. M.; Filice, M., New emerging bio-catalysts design in biotransformations. *Biotechnology Advances* **2015**, *33* (5), 605.
19. (a) Hilser, V. J.; Thompson, E. B., Intrinsic disorder as a mechanism to optimize allosteric coupling in proteins. *PNAS* **2007**, *104* (20), 8311; (b) Habchi, J.; Tompa, P.; Longhi, S.; Uversky, V. N., Introducing Protein Intrinsic Disorder. *Chem. Rev.* **2014**, *114*, 6561.
20. (a) Reed, B. J.; Locke, M. N.; Gardner, R. G., A Conserved Deubiquitinating Enzyme Uses Intrinsically Disordered Regions to Scaffold Multiple Protein Interaction Sites. *The Journal of Biological Chemistry* **2015**, *290*, 20601; (b) Ramírez, J.; Recht, R.; Charbonnier, S.; Ennifar, E.; Atkinson, R. A.; Travé, G.; Nominé, Y.; Kieffer, B., Disorder-To-Order Transition of MAGI-1 PDZ1 C-Terminal Extension upon Peptide Binding: Thermodynamic and Dynamic Insights. *Biochemistry* **2015**, *54* (6), 1327; (c) Uversky, V. N., The multifaceted roles of intrinsic disorder in protein complexes. *FEBS Letters* **2015**, *589* (19), 2498.
21. Motlagh, H. N.; Hilser, V. J., Agonism/antagonism switching in allosteric ensembles. *PNAS* **2012**, *109* (11), 4134.
22. Seo, M.-H.; Park, J.; Kim, E.; Hohng, S.; Kim, H.-S., Protein conformational dynamics dictate the binding affinity for a ligand. *Nature Communications* **2014**, *5*, 3724.
23. Peterson, P. E.; Smith, T. J., The structure of bovine glutamate dehydrogenase provides insights into the mechanism of allostery. *Structure* **1999**, *7*, 769–782.
24. Wacker, S. A.; Bradley, M. J.; Marion, J.; Bell, E., Ligand-induced changes in the conformational stability and flexibility of glutamate dehydrogenase and their role in catalysis and regulation. *Protein Science* **2010**, *19* (10), 1820.

25. Carrigan, J. B.; Engel, P. C., The structural basis of proteolytic activation of bovine glutamate dehydrogenase. *Protein Science* **2008**, *17*, 1346.
26. (a) Barbotin, J. N.; Breuil, M., Immobilization of Glutamate Dehydrogenase into proteic films: Stability and Kinetic Modulation effectors. *Biochimica et Biophysica Acta* **1978**, *525*, 18-27 ; (b) Barbotin, J.-N.; Thomasset, B., Immobilization of L-glutamate dehydrogenase into soluble cross-linked polymers. *Biochimica et Biophysica Acta* **1979**, *570*, 11-21 ; (c) Bigdeli, S.; Talasaz, A. H.; Stahl, P.; Persson, H. H. J.; Ronaghi, M.; Davis, R. W.; Nemat-Gorgani, M., Conformational Flexibility of a Model Protein Upon Immobilization on Self-Assembled Monolayers. *Biotechnology and Bioengineering* **2008**, *100* (1), 19-27.
27. Cordek, J.; Wang, X.; Tan, W., Direct Immobilization of Glutamate Dehydrogenase on Optical Fiber Probes for Ultrasensitive Glutamate Detection. *Anal. Chem.* **1999**, *71*, 1529-1533.
28. Doong, R.-a.; Shih, H.-m., Glutamate optical biosensor based on the immobilization of glutamate dehydrogenase in titanium dioxide sol-gel matrix. *Biosensors and Bioelectronics* **2006**, *22*, 185-191.
29. Blasi, L.; Longo, L.; Vasapollo, G.; Cingolani, R.; Rinaldi, R.; Rizzello, T.; Acierno, R.; Maffia, M., Characterization of glutamate dehydrogenase immobilization on silica surface by atomic force microscopy and kinetic analyses. *Enzyme and Microbial Technology* **2005**, *36*, 818-823.
30. Blasi, L.; Longo, L.; Pompa, P. P.; Manna, L.; Ciccarella, G.; Vasapollo, G.; Cingolani, R.; Rinaldi, R.; Rizzello, A.; Acierno, R.; Storelli, C.; Maffia, M., Formation and characterization of glutamate dehydrogenase monolayers on silicon supports. *Biosensors and Bioelectronics* **2005**, *21*, 30-40.
31. (a) Stalikas, C. D.; Karaynnis, M. I.; Tzouwara-Karayan, S., Immobilization of Glutamate dehydrogenase on glass derivatives: A method for the assay of glutamates in real samples with simplex optimized automated FIA-system *Talanta* **1994**, *41* (9), 1561-1567; (b) Petach, H. H.; Driscoll, J., Transparent Chitosan Derivatives for the Immobilization of Glutamate Dehydrogenase. *Biotechnology and Bioengineering* **1994**, *44*, 1018-1022; (c) Hourdou, M.-L.; Besson, F., Enzymatic Activities and Infrared Studies of Glutamate Dehydrogenase Immobilized on Langmuir-Blodgett Films *Biotechnology Techniques* **1995**, *9* (9), 643-648 ; (d) Jeffries, C.; Pasco, N.; Baronian, K.; Gorton, L., Evaluation of a thermophile enzyme for a carbon paste amperometric biosensor: L-glutamate dehydrogenase. *Biosensors & Bioelectronics* **1997**, *12* (3), 225-232; (e) Girard-Egrot, A. P.; Morélis, R. M.; Coulet, P. R., Bioactive nanostructure with glutamate dehydrogenase associated with LB films: protecting role of the enzyme molecules on the structural lipidic organization. *Thin Solid Films* **1997**, *292*, 282-289 ; (f) Gambhir, A.; Gerard, M.; Mulchandani, A. K.; Malhotra, B. D., Coimmobilization of Urease and Glutamate Dehydrogenase in Electrochemically Prepared Polypyrrole-Polyvinyl Sulfonate Films. *Applied Biochemistry and Biotechnology* **2001**, *96*, 249; (g) Pompa, P. P.; Blasi, L.; Longo, L.; Cingolani, R.; Ciccarella, G.; Vasapollo, G.; Rinaldi, R., Optical characterization of glutamate dehydrogenase monolayers chemisorbed on SiO₂. *Physical Review E* **2003**, *67*, 041902; (h) Longo, L.; Vasapollo, G.; Guascito, M. R.; Malitesta, C., New insights from X-ray photoelectron spectroscopy into the chemistry of covalent enzyme immobilization, with glutamate dehydrogenase (GDH) on silicon dioxide as an example. *Anal Bioanal Chem* **2006**, *385*, 146-152; (i) Bolivar, J. M.; Cava, F.; Mateo, C.; Rocha-Martín, J.; Guisán, J. M.; Berenguer, J.; Fernandez-Lafuente, R., Immobilization-stabilization of a new recombinant glutamate dehydrogenase from *Thermus thermophilus*. *Appl Microbiol Biotechnol* **2008**, *80*, 49-58; (j) Bolivar, J. M.; Rocha-Martín, J.; Godoy, C.; Rodrigues, R. C.; Guisan, J. M., Complete reactivation of immobilized derivatives of a trimeric glutamate dehydrogenase from *Thermus thermophilus*. *Process Biochemistry* **2010**, *45*, 107-113.
32. (a) El-Zahab, B.; Donnelly, D.; Wang, P., Particle-tethered NADH for production of methanol from CO₂ catalysed by coimmobilized enzymes. *Biotechnology and Bioengineering* **2008**, *99* (3), 508; (b) Zheng, M.; Zhang, S.; Ma, G.; Wang, P., Effect of molecular mobility on coupled enzymatic reactions involving cofactor regeneration using nanoparticle-attached

enzymes. *Journal of Biotechnology* **2011**, *154*, 274–280; (c) Zheng, M.; Su, Z.; Ji, X.; Ma, G.; Wang, P.; Zhan, S., Magnetic field intensified bi-enzyme system with in situ cofactor regeneration supported by magnetic nanoparticles. *Journal of Biotechnology* **2013**, *168* (2), 212–217.

33. Bolivar, J. M.; Mateo, C.; Rocha-Martin, J.; Cava, F.; Berenguer, J.; Fernandez-Lafuente, R.; Guisan, J. M., The adsorption of multimeric enzymes on very lowly activated supports involves more enzyme subunits: Stabilization of a glutamate dehydrogenase from *Thermus thermophilus* by immobilization on heterofunctional supports. *Enzyme and Microbial Technology* **2009**, *44*, 139–144.

34. Reisler, E.; Pouyet, J.; Eisenberg, H., Molecular Weights, Association, and Frictional Resistance of Bovine Liver Glutamate Dehydrogenase at Low Concentrations. Equilibrium and Velocity Sedimentation, Light-Scattering Studies,

and Settling Experiments with Macroscopic Models of the Enzyme Oligome. *Biochemistry* **1970**, *9* (15), 3095.

35. Zucca, P.; Sanjust, E., Inorganic Materials as Supports for Covalent Enzyme Immobilization: Methods and Mechanisms *Molecules* **2014**, *19*, 14139.

36. (a) Migneault, I.; Dartiguenave, C.; Bertrand, M. J.; Waldron, K. C., Glutaraldehyde: behavior in aqueous solution, reaction with proteins, and application to enzyme crosslinking *BioTechniques* **2004**, *37* (5), 790; (b) Barbosa, O.; Ortiz, C.; Berenguer-Murcia, Á.; Torres, R.; Rodrigues, R. C.; Fernandez-Lafuente, R., Glutaraldehyde in bio-catalysts design: a useful crosslinker and a versatile tool in enzyme immobilization. *RSC Adv.* **2014**, *4*, 1583.

37. Netto, C. G. C. M.; Nakamatsu, E. H.; Netto, L. E. S.; Novak, M. A.; Zuin, A.; Nakamura, M.; Araki, K.; Toma, H. E., Catalytic properties of thioredoxin immobilized on superparamagnetic nanoparticles *Journal of Inorganic Biochemistry* **2011**, *105* (5), 738-744.

38. Chauhan, G. S., Evaluation of nanogels as supports for enzyme immobilization. *Polymer International* **2014**, *63* (11), 1889.

39. (a) Hamilton, B. K.; Stockmeyer, L. J.; Colton, C. K., Comments on Diffusive and Electrostatic Effects with Immobilized Enzymes *J. theor. Biol.* **1973**, *41*, 547; (b) Tischer, W.; Wedekind, F., Immobilized Enzymes: Methods and Applications. In *Biocatalysis - From Discovery to Application*, Fessner, W.-D.; Archelas, A.; Demirjian, D. C.; Furstoss, R.; Griengl, H.; Jaeger, K.-E.; Morís-Varas, E.; Öhrlein, R.; Reetz, M. T.; Reymond, J.-L.; Schmidt, M.; Servi, S.; Shah, P. C.; Tischer, W.; Hide, F. W., Eds. 1999; Vol. 200, pp 95-126.

40. Xu, J.; Sun, J.; Wang, Y.; Sheng, J.; Wang, F.; Sun, M., Application of Iron Magnetic Nanoparticles in Protein Immobilization *Molecules* **2014**, *19*, 11465.

41. Govan, J.; Gun'ko, Y. K., Recent Advances in the Application of Magnetic Nanoparticles as a Support for Homogeneous Catalysts. *Nanomaterials* **2014**, *4* (2), 222.

42. Marques Netto, C. G. C. A., L. H.; Toma, H. E., Enantioselective transesterification catalysis by *Candida antarctica* lipase. *Tetrahedron. Asymmetry* **2009**, *20*, 2299-2304.

43. Garcia-Galan, C.; Berenguer-Murcia, Á.; Fernandez-Lafuente, R.; Rodrigues, R. C., Potential of different enzyme immobilization strategies to improve enzyme performance. *Adv. Synth. Catal.* **2011**, *353*, 2885.

44. Johnson, B. J.; Algar, W. R.; Malanoski, A. P.; Mario G. Ancona b, I. L. M., Understanding enzymatic acceleration at nanoparticle interfaces: Approaches and challenges. *Nano Today* **2014**, *9*, 102.

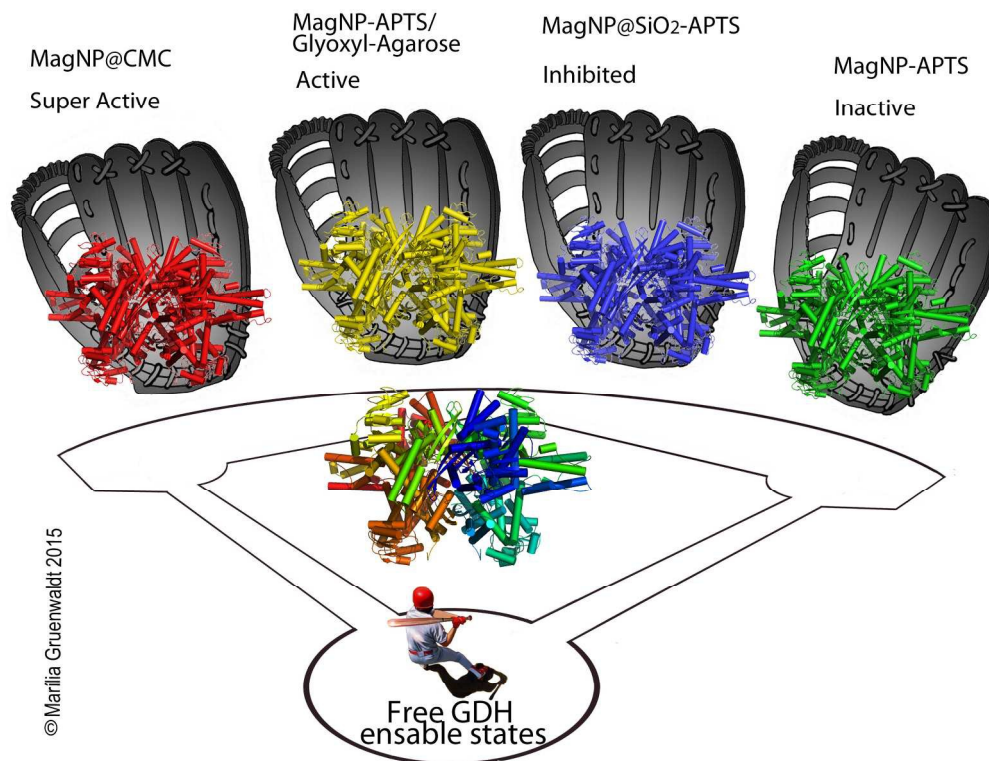
45. Mortimer, R. G.; Eyring, H., Elementary transition state theory of the Soret and Dufour effects. *Proceedings of the National Academy of sciences of the United States of America-Physical Sciences* **1980**, *77* (4), 1728-1731.

46. (a) Timasheff, S. N., Protein-Solvent Interactions and Protein Conformation *Acc. Chem. Res.* **1970**, *3* (2), 62; (b) Franks, F., Solvation interactions of proteins in solution. *Phil. Trans. R. Soc. Lond. B* **1977**, *278*, 89.

47. Sashi, P.; Yasin, U. M.; Balasubramanian, H.; Sree, M. U.; Ramakrishna, D.; Bhuyan, a. A. K., Preferential Water Exclusion in Protein Unfolding. *J. Phys. Chem. B* **2014**, *118*, 717.
48. Dijk, E. v.; Hoogeveen, A.; Abeln, S., The Hydrophobic Temperature Dependence of Amino Acids Directly Calculated from Protein Structures. *PLOS Computational Biology* **2015**, *11* (5), e1004277.
49. Castronuovo, G.; Elia, V.; Postiglione, C.; Velleca, F., Interactions of aminoacids in concentrated aqueous solutions of urea or ethanol. Implications for the mechanism of protein denaturation. *Thermochimica Acta* **1999**, *339*, 11.
50. Low, P. S.; Bada, J. L.; Somero, G. N., Temperature Adaptation of Enzymes: Roles of the Free Energy, the Enthalpy and the Entropy of activation. *Proc. Nat. Acad. Sci. USA* **1973**, *70* (2), 430-432.
51. *Protein Adaptation in Extremophiles*; 2008.
52. Weiss, J. N., The Hill equation revisited: uses and misuses. *The FASEB Journal* **1997**, *11* (11), 835.
53. Krupyanko, V. I., An additional Possibility of Using the Hill Coefficients. *4* **2015**, *7* (Eur. Chem. Bull.), 340.
54. Petach, H. H.; Driscoll, J., Transparent Chitosan Derivatives for the Immobilization of Glutamate Dehydrogenase. *Biotechnology and Bioengineering* **1994**, *44*, 1018-1022.
55. Tamayo, J.; García, R., Deformation, Contact Time, and Phase Contrast in Tapping Mode Scanning Force Microscopy. *Langmuir* **1996**, *12*, 4430.
56. Chikisev, A. Y.; Otto, C.; Brandt, N. N.; Molodozhenya, V. V.; Sakodynskaya, I. K.; Greve, J.; Koroteev, N. I., Function-related conformational changes of protein molecules revealed by Raman spectroscopy. In *Spectroscopy of Biological Molecules: New Directions*, Greve, J.; Puppels, G. J.; Otto, C., Eds. Kluwer Academic Publishers: Netherlands, 1999.
57. (a) Babbitt, S. E.; Francisco, B. S.; Mendez, D. L.; Lukat-Rodgers, G. S.; Rodgers, K. R.; Bretsnyder, E. C.; Kranz, R. G., Mechanisms of Mitochondrial Holocytochrome c Synthase and the Key Roles Played by Cysteines and Histidine of the Heme Attachment Site, Cys-XX-Cys-His. *The Journal of Biological Chemistry* **2014**, *289* (42), 28795–28807; (b) Zhao, J.; Moretto, J.; Le, P.; Franzen, S., Measurement of Internal Substrate Binding in Dehaloperoxidase– Hemoglobin by Competition with the Heme–Fluoride Binding Equilibrium. *J. Phys. Chem. B* **2015**, *119*, 2827–2838.
58. Maiti, N. C.; Apetri, M. M.; Zagorski, M. G.; Carey, P. R.; Anderson, V. E., Raman Spectroscopic Characterization of Secondary Structure in Natively Unfolded Proteins: a-Synuclein. *J. Am. Chem. Soc.* **2004**, *126*, 2399-2408.
59. Bunaciu, A. A.; Aboul-Enein, H. Y.; Hoang, V. D., Raman Spectroscopy for Protein Analysis. *Applied Spectroscopy Reviews* **2015**, *50*, 377.
60. Carey, P. R.; Storer, A. C., Characterization of transient enzyme-substrate bonds by resonance raman spectroscopy. *Ann. Rev. Biophys. Bioeng.* **1984**, *13*, 25-49.
61. Dzwolak, W.; Smirnovas, V., A conformational α -helix to β -sheet transition accompanies racemic self-assembly of polylysine: an FT-IR spectroscopic study. *Biophysical Chemistry* **2005**, *115*, 49.
62. Chi, Z.; Ashe, S. A., UV Resonance Raman Determination of Protein Acid Denaturation: Selective Unfolding of Helical Segments of Horse Myoglobin. *Biochemistry* **1998**, *37*, 2865-2872.
63. Barron, D. L.; Blanch, E. W.; Hecht, L., Advances in Protein Chemistry. In *Unfolded Proteins*, Academic Press: San Diego, California, 2002; Vol. 62.
64. Li, M.; Li, C.; Allen, A.; Stanley, C. A.; Smith, T. J., The structure and allosteric regulation of glutamate dehydrogenase. *Neurochem Int.* **2011**, *59* (4), 445.
65. Fisher, H. F.; Tally, J., Isoergonic Cooperativity in Glutamate Dehydrogenase Complexes: A New Form of Allostery. *Biochemistry* **1997**, *36*, 10807-10810.
66. Smith, E. L.; Landon, M.; Piszkiwicz, D.; Brattin, W. J.; Langley, T. J.; Melamed, M. D., Bovine Liver Glutamate Dehydrogenase: Tentative Amino Acid Sequence; Identification of a

- Reactive Lysine; Nitration of a Specific Tyrosine and Loss of Allosteric Inhibition by Guanosine Triphosphate. *Proceedings of the National Academy of Sciences* **1970**, *67* (2), 724-730.
67. Stanley, C. A., Regulation of glutamate metabolism and insulin secretion by glutamate dehydrogenase in hypoglycemic children. *Am J Clin Nutr* **2009**, *90* (3), 8625.
68. Smith, T. J.; Stanley, C. A., Untangling the glutamate dehydrogenase allosteric nightmare. *Trends in Biochemical Sciences* **2008**, *33* (11), 557.
69. Banerjee, S.; Schmidt, T.; Fang, J.; Stanley, C. A.; Smith, T. J., Structural Studies on ADP Activation of Mammalian Glutamate Dehydrogenase and the Evolution of Regulation. *Biochemistry* **2003**, *42*, 3446-3456.
70. Wacker, S. A.; Bradley, M. J.; Marion, J.; Bell, E., Ligand-induced changes in the conformational stability and flexibility of glutamate dehydrogenase and their role in catalysis and regulation. *Protein Science* **2010**, *19*, 1820.
71. Guisán, J. M.; Alvaro, G.; Fernandez-Lafuente, R.; Rosell, C. M.; Garcia, J. L.; Tagliani, A., Stabilization of heterodimeric enzyme by multipoint covalent immobilization: Penicillin G acylase from *Kluyvera citrophila*. *Biotechnology and Bioengineering* **1993**, *42* (4), 455.
72. Mateo, C.; Abian, O.; Fernandez-Lafuente, R.; Guisan, J. M., Increase in conformational stability of enzymes immobilized on epoxy-activated supports by favoring additional multipoint covalent attachment. *Enzyme and Microbial Technology* **2000**, *26* (7), 509.
73. Grazú, V.; Abian, O.; Mateo, C.; Batista-Viera, F.; Fernández-Lafuente, R.; Guisán, J. M., Stabilization of enzymes by multipoint immobilization of thiolated proteins on new epoxy-thiol supports. *Biotechnology and Bioengineering* **2005**, *90* (5), 597.
74. Manrich, A.; Komesu, A.; Adriano, W. S.; Tardioli, P. W.; Giordano, R. L. C., Immobilization and Stabilization of xylanase by multipoint covalent attachment on agarose and on chitosan supports. *Appl. Biochem. Biotech* **2010**, *161*, 455.
75. Motlagh, H. N.; Wrabl, J. O.; Li, J.; Hilser, V. J., The ensemble nature of allostery. *Nature* **2014**, *508*, 331.
76. Smith, T. J.; Schmidt, T.; Fang, J.; Wu, J.; Siuzdak, G.; Stanley, C. A., The Structure of Apo Human Glutamate Dehydrogenase Details Subunit Communication and Allostery. *J. Mol. Biol.* **2002**, *318*, 765-777.
77. Cooper, A.; Dryden, D. T. E., Allostery without conformational change. *Eur. Biophys. J.* **1984**, *11*, 103.
78. Reichheld, S. E.; Yu, Z.; Davidson, A. R., The induction of folding cooperativity by ligand binding drives the allosteric response of tetracycline repressor. *PNAS* **2009**, *106* (52), 22263.
79. Luque, I.; Freire, E., Structural Stability of Binding Sites: Consequences for binding affinity and allosteric effects. *Proteins: Structure, Function and Genetics Suppl* **2000**, *4*, 63.
80. Dyson, H. J.; Wright, P. E., Coupling of folding and binding for unstructured proteins. *Current Opinion in Structural Biology* **2002**, *12*, 54.
81. Petit, C. M.; Zhang, J.; Sapienza, P. J.; Fuentes, E. J.; Lee, A. L., Hidden dynamic allostery in a PDZ domain. *PNAS* **2009**, *206* (43), 18249.
82. Frederick, K. K.; Marlow, M. S.; Valentine, K. G.; Wand, A. J., Conformational entropy in molecular recognition by proteins. *Nature* **2007**, *448*, 325.
83. Ogorzalek, T. L.; Wei, S.; Liu, Y.; Wang, Q.; Brooks, C. L.; Chen, Z.; Marsh, E. N. G., Molecular-Level Insights into Orientation-Dependent Changes in the Thermal Stability of Enzymes Covalently Immobilized on Surfaces. *Langmuir* **2015**, *31*, 6145.
84. Cioni, P.; Strambini, G. B., Dynamical Structure of Glutamate Dehydrogenase as Monitored by Tryptophan Phosphorescence : Signal Transmission Following Binding of Allosteric Effectors. *J. Mol. Biol.* **1989**, *207*, 237.

Immobilized ensemble states results



199x173mm (300 x 300 DPI)